An Evaluation and Comparison of Vertical Profile Data From the VISSR Atmospheric Sounder (VAS)

Gary J. Jedlovec

NASA

An Evaluation and Comparison of Vertical Profile Data From the VISSR Atmospheric Sounder (VAS)

Gary J. Jedlovec

George C. Marshall Space Flight Center
Marshall Space Flight Center, Alabama

ACKNOWLEDGMENTS

TABLE OF CONTENTS

LIST OF ILLUSTRATIONS

LIST OF TABLES

TECHNICAL PAPER

AN EVALUATION AND COMPARISON OF VERTICAL PROFILE DATA FROM THE VISSR ATMOSPHERIC SOUNDER (VAS)

I. INTRODUCTION

In the fall of 1980, the first VISSR Atmospheric Sounder (VAS) was launched into geostationary orbit with the GOES-4 satellite. VAS is a 12 channel radiometer capable of obtaining imagery of the thermal and moisture structure of the atmosphere at short time intervals and small spatial scales over a rather large geographic region. Since then, two other VAS instruments have been launched into geostationary orbit. Due to satellite configurations and limitations of the ground system, VAS data can only be collected from one satellite at a time, making the routine collection of VAS data somewhat limited.

Much imagery has been collected and archived from VAS on these three satellites over the last several years, however, only a small portion of this has been used by the atmospheric science community. This data is readily available to only a few users with sophisticated computer equipment to ingest and process the vast quantities of data. For the past several years, the Satellite Field Service Station (SFSS), the National Severe Storms Forecast Center (NSSFC), and the Cooperative Institute for Meteorological Satellite Studies (CIMSS) at the University of Wisconsin have participated in the NOAA Operational VAS Assessment program (NOVA) by utilizing imagery and satellite sounding data in quasi-real time [1]. The assessment was not continuous during this time due to many problems related to satellite availability. However, the potential utility of VAS imagery and sounding products was demonstrated. Results also indicate that temperature and height fields from VAS were similar to those of the rawinsonde but dewpoint values were unreliable especially in the lower levels. Derived values of precipitable water and stability were useful to calculate time derivatives (avoiding absolute magnitudes) but are difficult to calculate and monitor over a regional area given the irregular spacing of the VAS retrievals and the movement of the sounding locations with time due to cloudiness.

There has been relatively few studies which examine the accuracy of the temperature and moisture information contained in this data and extracted in the retrieval process. This is mainly due to the lack of appropriate ground truth data to evaluate the performance of the instrument and the accuracy of the retrieval algorithms. Menzel, et al. [2] performed an inflight evaluation of radiance data shortly after the first VAS was launched. They found discernable time variability in retrieved VAS soundings with rawinsonde/satellite profiles typically within $1°$ to $2°C$ of each other and maximum deviations of $5°C$ occurring from time to time. Chesters, et al. [3] performed a simulation experiment in order to evaluate mesoscale features resolvable by VAS using a minimum information linear regression scheme. Their study simulated VAS radiances from a dependent rawinsonde data set (six NSSL storm cases in Oklahoma) and then applied the statistical relationships to four other cases. Results indicated that by using locally conditioned regression matrices, temperature errors ranged from $1°$ to $2°C$ at all levels and mixing ratio values were retrieved to within 25 percent of the rawinsonde value. Horizontal fields of integrated parameters (thickness and precipitable water) showed good correlation to the ground truth with a slight reduction in the magnitude of the gradient information. Lee, et al. [4] investigating the impact of conventional surface data upon VAS regression retrievals concluded that the absolute temperature and dewpoint accuracies using VAS plus surface information were from $1°$ to $2°C$ and $1°$ to $6°C$, respectively. These accuracies showed a substantial improvement over those without surface data and regional rawinsonde measurements for the training data set.

Studies which have made use of VAS imagery and sounding products for diagnostic analysis (e.g., Smith [5]; Chesters, et al. [6]; and Petersen, et al. [7] and for nowcasting applications (e.g., Anthony and Wade [1] and Smith and Zhou [8]) depended heavily on VAS information at scales of motion (temporal and spatial) at which there are no conventional measurements to verify the satellite observations. Much of the validation of mesoscale features in the VAS data consisted of actual severe storm events or convective development serving as ground truth. When corresponding synoptic scale rawinsonde data were present, discrepancies were explained as acceptable (due to temporal differences) or below the resolution of the ground truth measurements.

In the spring of 1982, the NASA's Marshall Space Flight Center, in cooperation with Texas A and M University, conducted a field experiment to obtain ground truth data at the scales resolvable by VAS (Hill and Turner [9]). The experiment consisted of making rawinsonde observations over a regional and mesoscale network in the Midwest and Texas, respectively, at three-hour intervals during several observational periods which corresponded to VAS measurements. It is the purpose of this paper to describe the results of a case study which evaluated the accuracy and representativeness of VAS sounding data from three different retrieval algorithms utilizing the satellite and rawinsonde data from this experiment. Mean and standard deviations of the differences between each data set will be presented along with vertical profiles and horizontal cross sections of basic and derived parameters. An analysis of the first guess and apriori information will be presented in order to infer what improvement is being made with the VAS radiances. Finally, errors in both the rawinsonde and satellite radiances will be evaluated in light of the rawinsonde-satellite discrepancies.

II. INSTRUMENT DESCRIPTION AND NETWORK DESIGN

The VISSR Atmospheric Sounder (VAS) is passive infrared radiometer which senses radiation emitted by the atmospheric and the earth's surface in 12 spectral bands from 3.7 to 15.0 μm. Characteristics of these channels are given in Table 1 while Figure 1 displays the weighting functions (indicating the layer of the atmosphere from which radiation is received by VAS). VAS imagery is collected in scan line as the GOES satellite spins in a west to east direction. The resolution of each field-of-view (FOV) along a scan line is 7 or 14 km at nadar depending on whether the small or large detectors are used. Only with the large detectors (14 km FOV) can the atmosphere be sampled in all 12 channels. The GOES spacecraft operating in the normal VISSR mode scans the entire disk of the earth in 18 min. Since VAS has multiple channel capabilities and requires additional spins on the same scan line to increase the signal to noise ratio in some channels, time requirements for VAS to scan a smaller section, usually an area the size of the continental United States. Within these constraints, VAS can be used to scan this area repeatedly at intervals of 10 to 20 min but is typically used every 1 to 3 hr. This frequency and coverage allows for sounding production at resolutions far greater than the conventional observing networks. Additional information about VAS instrument characteristics can be found in Menzel, et al. [2], Smith, et al. [10], and Chesters, et al [3].

For satellite sounding purposes the dwell sound (DS) mode of VAS is used whereby multiple samples of upwelling radiances are averaged together to achieve a higher signal-to-noise ratio required for sounding quality radiances. Averaging of several adjacent FOVs (horizontal averaging) may be employed to further improve the quality of this data. Because of this averaging and the spacing of the retrievals, temperature and moisture profiles are described as having a horizontal resolution of 20 to 75 km. The vertical resolution of these profiles is limited by the broadness of the weighting functions (Fig. 1) and is roughly on the order of 200 mb.

TABLE 1. VAS CHANNEL CHARACTERISTICS

VAS CH =	FILT CENT ν	FILT CENT cm⁻¹	FILT BAND cm⁻¹	PURPOSE FOR SOUNDING	MAIN ABS GAS	OTHER SIGNIF EFFECTS	SAMPLE NOISE ±°K
1	14.7	678	10	TEMP	CO_2	O_3	5.3
2	14.5	691	16	TEMP	CO_2	O_3	2.2
3	14.3	699	16	TEMP	CO_2	O_3	1.8
4*	14.0	713	20	TEMP	CO_2	O_3	1.2
5*	13.3	750	20	TEMP	CO_2	H_2O	1.0
6	4.5	2209	45	TEMP + CLOUD	N_2O	SUN	1.6
7*	12.7	787	20	MOISTURE	H_2O	CO_2	1.0
8*	11.2	892	140	SURFACE	–	$H_2O + CO_2$	0.1
9*	7.3	1370	40	MOISTURE	H_2O	–	3.4
10*	6.8	1467	150	MOISTURE	H_2O	–	1.6
11	4.4	2254	40	TEMP + CLOUD	CO_2	SUN	6.7
12	3.9	2540	140	SURFACE	–	SUN + H_2O	0.8

*AVAILABLE AT 7 km (NADIR VIEW) RESOLUTION.
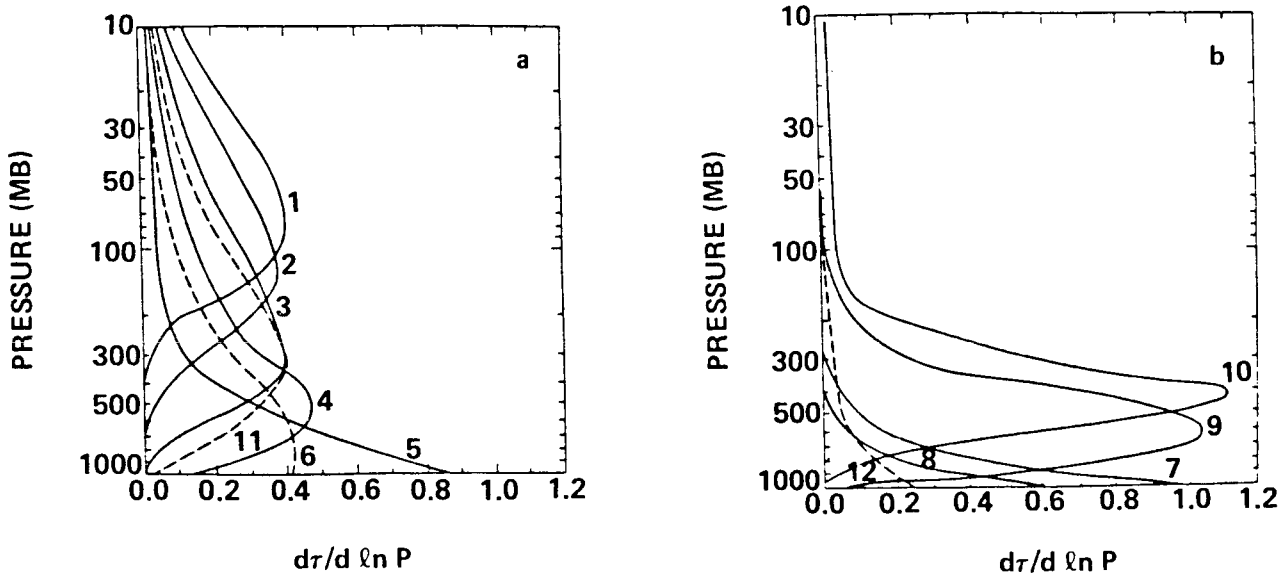
Figure 1. VAS weighting functions for the (a) CO_2 absorption channels, and (b) water vapor and atmospheric window channels.

In order to evaluate VAS vertical profile information having fine horizontal resolution described above, a special experiment was designed to collect ground truth rawinsonde measurements at a similar scale. The 1982 AVE/VAS Ground Truth Field Experiment [9] collected rawinsonde data at 24 National Weather Service (NWS) sites and 12 special network sites for four different 18 hr observation periods in the spring of 1982 (Fig. 2). During each of these observation periods, three-hourly rawinsonde measurements were made from these sites which corresponded rather closely to the time of the VAS dwell sound satellite data. Operating constraints limited the flexibility of the collection periods and unfortunately a wide variety of cases were not collected. In the most useful case, the regional and mesoscale network were under clear skies for a number of time periods. This case will be discussed in Section III.
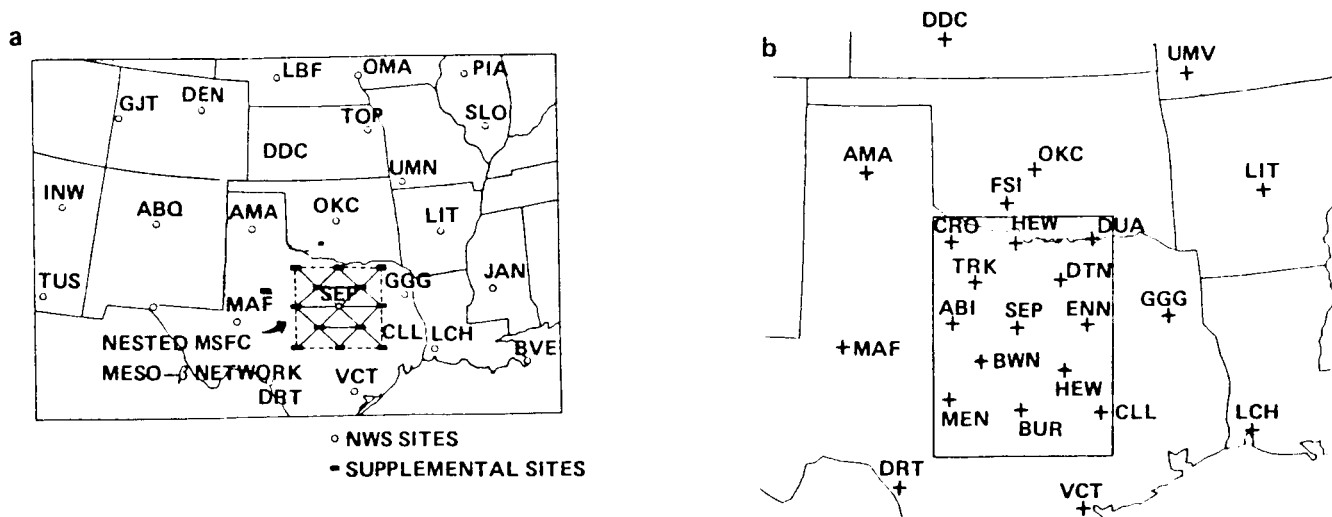
Figure 2. AVE/VAS rawinsonde sites for the (a) regional and special network, and
(b) special (mesoscale) sites used in the objective analysis and comparisons.
The rectangular box locates the hour domain of the 10 x 13 grid region.

III. DATA

A. Vertical Profile Information

Two basic types of data were used in the study; namely, rawinsonde and VAS sounding data for the 6-7 March 1982 AVE/VAS experiment day. The VAS sounding data available for this period consisted of three data sets, each composed of soundings at 1100, 1435, 1735, 2035, and 2335 GMT (beginning satellite scan times). The first satellite data set contained vertical profiles of geopotential height, temperature, and dewpoint temperature at 10 standard levels and was produced using a scheme similar to the one used by Smith [11]. The scheme is a physical one where an iterative solution is employed and LFM model output is used as first guess information. Radiance data from a maximum of 25 (minimum of 4) 14 km FOVs were averaged together before the retrievals were made. Also, some partly cloudy retrievals were acquired using the N-star technique [12]. These soundings will be referred to as "physical" retrievals.

The second data set is similar to the previous one except an analytic solution is employed after the iterative physical retrievals are obtained in order to provide more vertical structure to the satellite profiles [5]. A similar number of clear fields of view were averaged together depending on cloud cover. No attempt was made to retrieve partly cloudy soundings. The soundings will be called "modified physical" retrievals.

The third set of VAS soundings was produced using a linear regression scheme as described by Lee, et al. [4]. This method uses a local rawinsonde data set (NWS soundings at 1200 and 0000 GMT, 6 and 7 March 1982, respectively) and surface data to determine statistical relationships between the radiance measurements and the structure of the atmosphere at co-located rawinsonde and surface sites. These relationships were then applied to the observed radiance measurements to derive temperature and moisture profiles over the entire field for each of the five time periods. Radiance information from five over-lapping fields of view were averaged together before the regression retrievals were made. This is considerably less spatial averaging than with the physical retrievals. This data set will be denoted as "regression" soundings.

4

In all three data sets, soundings had a horizontal spacing of approximately 50 to 100 km over the entire cloud-free region of Texas, Oklahoma, and surrounding states. This spacing (resolution) should not be confused with the area over which radiances were averaged before the production of satellite retrievals as discussed above.

The rawinsonde data used in the evaluation consisted of the basic thermodynamic parameters (geopotential height, temperature, and dewpoint) at 50 mb increments from the surface up to 100 mb [13]. These rawinsonde data were carefully checked and edited as part of the reduction process. The rawinsonde locations of interest are shown in Figure 2. The spacing of these sites is roughly 125 km over central Texas providing detailed mesoscale resolution of atmospheric features. The nominal release times of the rawinsinde data were 1200, 1500, 1800, and 2100 GMT on 6 March 1982 and 0000 GMT on 7 March 1982.

B. Synoptic and Mesoscale Conditions for 6 March 1982

The 6-7 March 1982 case was used for extensive ground truth comparisons because of a large region of predominately cloud-free skies over the special network region. Figure 3 presents the surface, 500 mb, and 300 mb analysis at 1200 GMT 6 March and 0000 GMT 7 March 1982. At 1200 GMT, a surface low pressure center was present along the Gulf Coast with a stationary front extending southwestward into Mexico. Behind this front, a shallow high pressure area was centered over western Oklahoma. To the north, a cold front, extending from a low up in Canada, was pushing south through the Upper Plain states. The thermal gradient over the central portion of the region was quite strong with a 15°C gradient over Texas and a similar one over the Central Plains. The western half of the regional network was predominantly cloud-free at this time (not shown) and low clouds persisted in east Texas while convective clouds with thunderstorm activity were present over Louisiana, Arkansas, and Missouri. Several inches of snow were on the ground in portions of Oklahoma and west Texas but melted during the afternoon hours.

Aloft, a large amplitude trough at 500 mb was positioned over the regional network in a northeast-southwest orientation (Fig. 3a). This trough was well defined by the height and wind shear field with a strong thermal gradient through northwest Texas and Oklahoma. A very narrow wind maximum was present in the southern portion of the region with maximum winds exceeding 35 ms^{-1} at Stephenville and Tucson. At 300 mb, a closed low circulation was present over eastern Nebraska with a well defined trough extending back into New Mexico. A strong jet streak was present over the border of Mexico and the Southwest states with maximum winds in excess of 60 ms^{-1}. This feature with its associated circulation patterns had a major impact on the atmospheric processes which occurred in the region.

By 0000 GMT 7 March 1982, the synoptic charts (Fig. 3b) indicate significant movement of the atmospheric features over the last 12 hr. The surface low pressure located over the Gulf Coast moved eastward as did the showers and thunderstorms associated with it. The cold front over the Northern Plains moved south through Kansas and Nebraska bringing even colder and drier air into the region. No precipitation and just scattered clouds were associated with the front in this region. Surface temperatures rose considerably over the regional network during the day due to solar heating and a substantial temperature gradient still existed off the Gulf Coast and in the western portion of the experiment region.

At 500 mb, the large amplitude wave shifted slightly to the east but the southern extension of the trough rotated rapidly through the mesoscale network by 0000 GMT. The strong thermal gradient

Figure 3. Surface and upper level synoptic charts at (a) 1200 GMT 6 March 1982, and (b) 0000 GMT 7 March 1982. Bold (dark) contours indicate pressure in millibars at the surface and geopotential heights in meters aloft. Thin (light) contours indicate temperature in °C for the surface and 500 mb and isotachs at 300 mb in m/sec.

present at 1200 GMT (Fig. 3a) moved through central Texas and was positioned over southern and eastern Texas just beyond the mesoscale network (Fig. 2). The progression of this cold feature through the mesoscale rawinsonde network was well captured by the three-hourly data and is discussed below. The 300 mb diagram shows an equally rapid shift of the trough line through west Texas. A well defined jet streak is present at the base of the trough with winds still exceeding 60 ms^{-1}.

The three-hourly data collected from the mesoscale network over Texas (Fig. 2) captured many atmospheric features as they propagate through the network. Two of the most prominent are the low-level drying behind the front and the propagation of a small pocket of cold mid-tropospheric air over the region. Figure 4 presents the 850 mb temperature and dewpoint depression analysis for five consecutive times from 1100 through 2345 GMT. It is useful to be reminded of the frontal positions
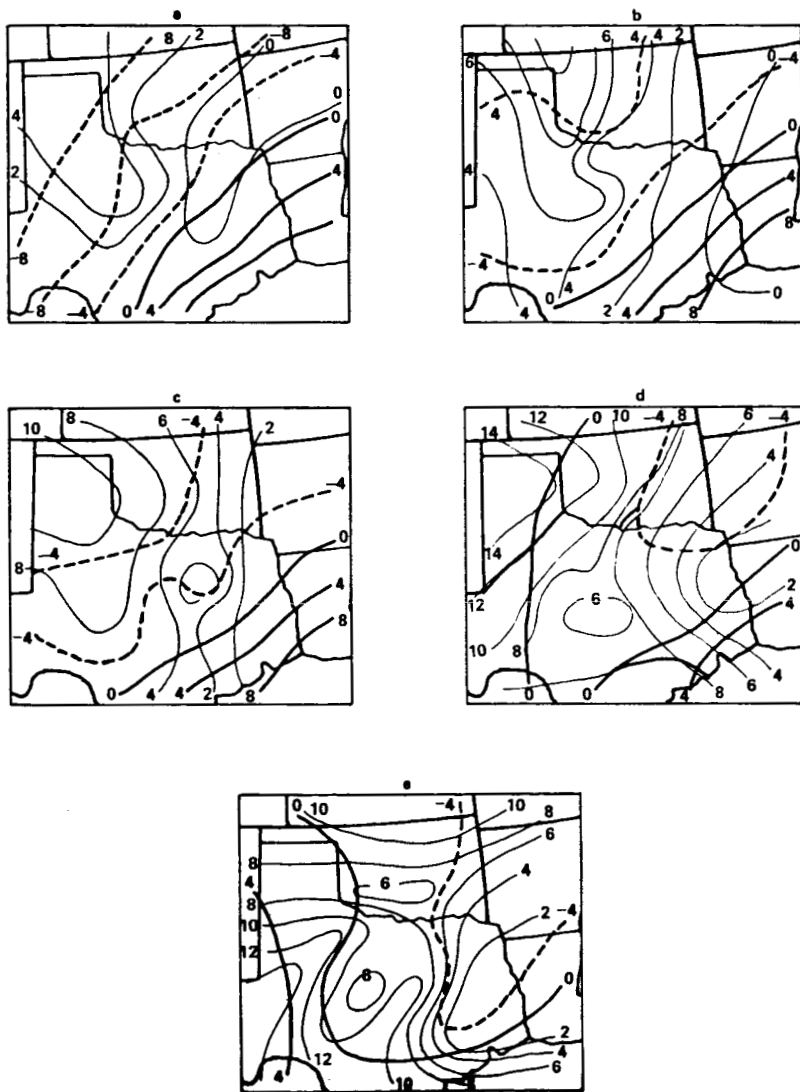
Figure 4. Mesoscale analysis of temperature (bold lines) and dewpoint depression (thin lines) for 850 mb at (a) 1100 GMT, (b) 1445 GMT, (c) 1745 GMT, (d) 2045 GMT, and (e) 2345 GMT 6 March 1982. Units are in °C.

7

described above (Fig. 3a and 3b) and the cloud cover at 1800 GMT presented in Figure 5. The 850 mb temperature fields (heavy lines) indicate a somewhat similar structure as the surface fields with a northwest-southeast temperature gradient behind the frontal zone. The front at 850 mb is estimated to be approaching the Gulf Coast at 1100 GMT. The coldest temperatures exist in west Texas and Oklahoma. This pattern weakens during the day with the solar heating dominating the lowest layer in the cloud-free regions. This is apparent between 1745 and 2045 GMT when the entire mesoscale network becomes cloud-free. By 2345 GMT the temperature gradient has almost reversed with warm air residing over west Texas and a moderate gradient extending east through the special network. The dewpoint depression values (thin lines) indicated a saturated or nearly saturated lowest layer in the eastern portions of the mesoscale region. This moist feature moves eastward with the cloud cover (Fig. 5) as drier air with dewpoint depression values greater than 10°C entering the mesoscale region by 2045 GMT. Very fine scale structure is observed where mesoscale moisture residuals are present at this level.
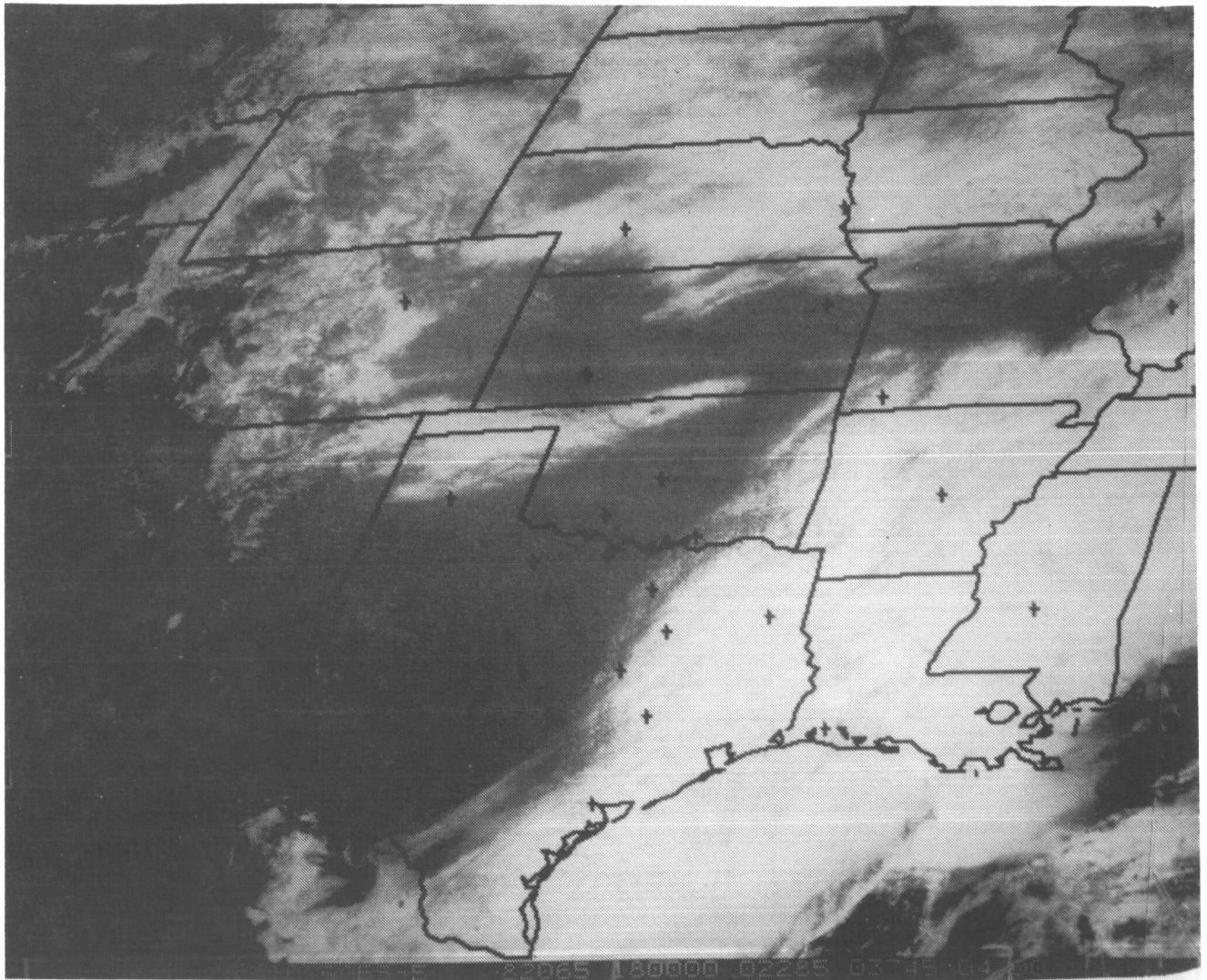
Figure 5. Visible image from the GOES East satellite at 1800 GMT 6 March 1982.
Rawinsonde sites are superposed on the image.

8

The 500 mb analysis over the mesoscale region is presented in Figure 6 at three-hourly intervals. The mesoscale (time and space) data serve to more accurately define the position and movement of the trough and temperature field through the Texas and Oklahoma region than do the conventional synoptic scale data shown in Figure 3. These data nicely pinpoint the 500 mb temperature minimum located immediately behind the trough line as it progresses through the network. This feature is important not only to the maintenance of the system but also because it represents an atmospheric feature which could possibly be resolved by VAS.
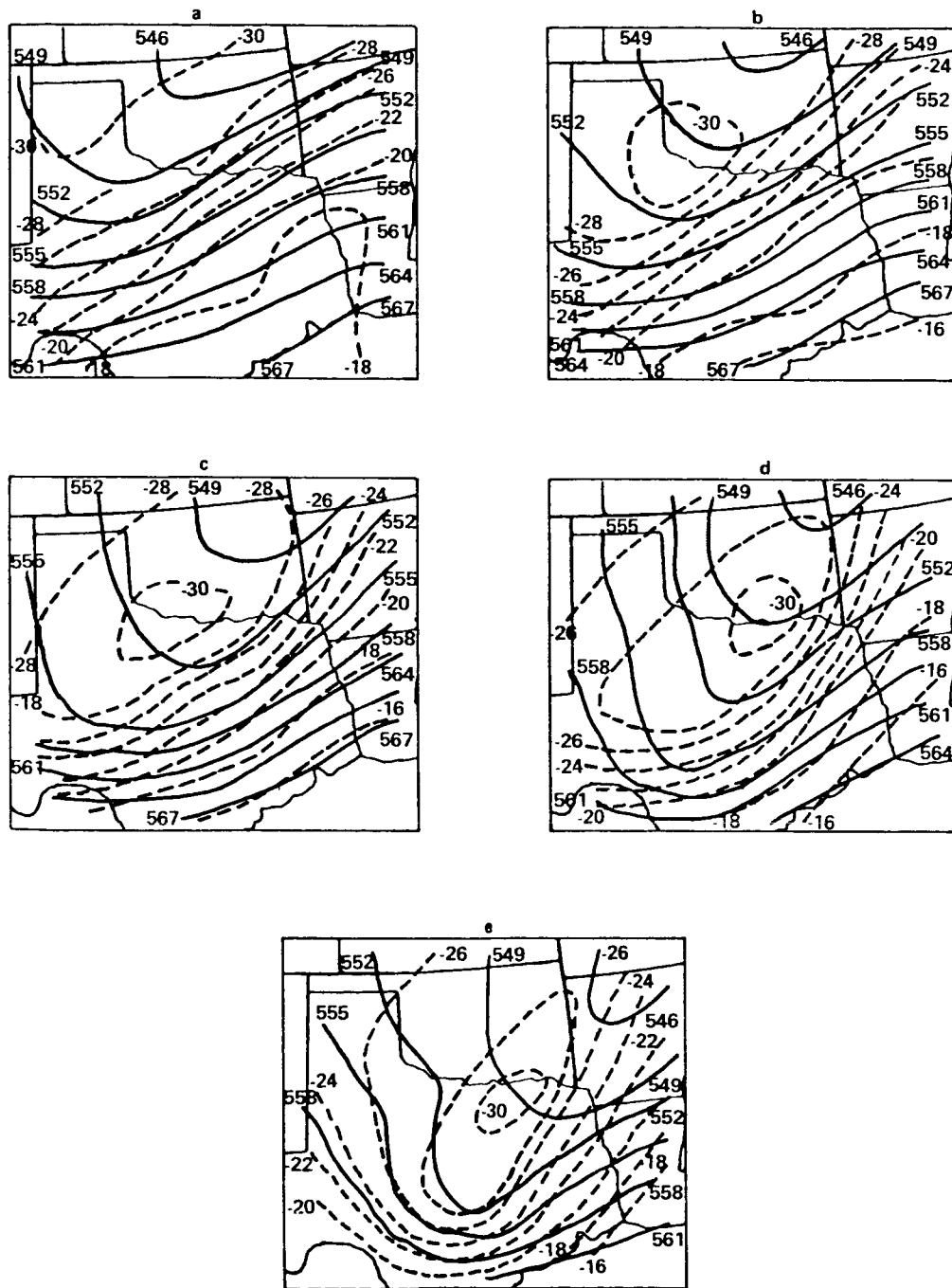
Figure 6. Mesoscale analysis of geopotential height (solid lines) and temperature (dashed lines) at 500 mb for (a) 1100 GMT, (b) 1445 GMT, (c) 1745 GMT, (d) 2045 GMT, and (e) 2345 GMT 6 March 1982. Units are in meters and °C for the height and temperatures, respectively.

IV. METHODOLOGY

A. Time and Space Adjustments

Rawinsonde and satellite soundings are rarely co-located in space nor taken at the same time thus making comparisons between them difficult to interpret. To overcome this problem, special procedures were used to make the rawinsonde and satellite data sets more consistent. First the ground truth rawinsonde data adjusted to a common release time (10 min after the beginning satellite scan time) using a scheme described by Fuelberg and Jedlovec [14]. The new rawinsonde times in this study are 1100, 1445, 1745, 2045, and 2345 GMT on 6 March 1982. This procedure provided rawinsonde and satellite data which were valid at the same times at all levels of the atmosphere. The satellite profiles were interpolated to 50 mb increments from the supplied standard pressure level data. In the case of the regression soundings, geopotential heights were calculated from the temperature and moisture profiles using the hypsometric equation. The rawinsonde and satellite data then were both objectively analyzed to a 10 x 13 uniform grid over central Texas with the balloon position (radiosonde) being recalculated at every level in the vertical. This procedure helped to eliminate spatial discrepancies between the data since the same grid was used for all data sets (Fig. 2b). The same objective analysis scheme weighting parameters were utilized in each case so that the potential for detail in the gridded fields was similar at each level, time, and for each data set. In the cases where part of the analysis region was void of satellite soundings due to clouds (mainly 1100 and 1445, but to a small extent at 1745) grid point values were not determined in these regions to avoid misrepresenting atmospheric features.

The procedures followed in this evaluation and described above have provided three sets of satellite data and a set of ground truth rawinsonde data on constant pressure surfaces at 50 mb increments from the surface to 100 mb. In addition to the basic parameters (height, temperature, and dewpoint), gridpoint values of total precipitable water, thickness (over three layers of the atmosphere) and gradient and time change information were calculated and subjected to an evaluation.

B. Statistical Calculations

Utilizing identically gridded rawinsonde and satellite data, mean differences and standard deviations of the differences between the rawinsonde and each satellite grid were calculated. Although each point is not an independent value, enough observations (greater than 15 for rawinsonde and greater than 30 for the satellite soundings) were allowed to influence the gridded field such that statistical significance was maintained. The statistical parameters were calculated only over the regions of the grid where valid observations existed, thereby avoiding misleading results due to cloudy regions of the grid area. Additionally, horizontal fields of basic and derived parameters and vertical profiles of grid mean values were analyzed. The results of this evaluation are presented in Section V.

V. RESULTS

A. Statistical Comparison — All-Times Combined

Tables 2 through 6 present the mean differences and standard deviations of the differences between the rawinsonde and each satellite data set for all five time periods combined. The total number of grid points used differs from one satellite data set to another due to the location of the soundings w.r.t. the cloud fields. The grid point numbers do not vary enough, however, to make a significant

10

difference when results from one retrieval algorithm are compared to another. Although the all-times results mask the diurnal variability, they serve as a representative set of numbers for a general impression of the quality of the data and to be used by others for comparison with other remote sensing instruments. The diurnal variability will be addressed in a following section.

Mean temperature differences (Table 2) for all-times combined indicate the over-all temperature bias in each VAS data set relative to the rawinsonde measurements. Since the satellite grid point values are subtracted from the ground truth rawinsonde values (Rao - Sat), a negative (positive) number indicates a warm (cold) bias. The bias pattern is similar for each retrieval method with a warm bias in the lowest 150 mb capped by a cold bias from 800 mb to roughly 650 mb. The magnitude of the warm bias is 2° to 3°C for each scheme. The cold bias in the low levels is greatest in the modified physical retrievals with values as high as 2.6°C at 750 mb. Bias values for this layer remain below 1.0°C for the physical and regression schemes. In the middle and upper troposphere (600 to 300 mb), a fairly strong warm bias exists in all retrieval schemes with values ranging from 1° to 2°C. The maximum biases occur around 400 mb. Above 300 mb, the physical retrievals maintain a warm bias while the modified physical and regression schemes vary but generally indicate a cold bias. The bias patterns indicated in the entire column seem to reflect the inability of the VAS instrument and retrieval schemes to detect the detailed vertical structure in the rawinsonde data (discussed later). Despite these temperature biases, the standard deviation of the difference fields show very similar patterns for all three data sets. The values range from 1° to 2°C with maximum deviations occurring around 450 to 500 mb and 250 mb. A secondary maximum exists in the very lowest layer where the warm/cold bias couplet exists.

TABLE 2. MEAN AND STANDARD DEVIATION OF THE DIFFERENCES BETWEEN THE RAWINSONDE AND SATELLITE GRID POINT TEMPERATURE VALUES FOR A COMPOSITE OF FIVE TIME PERIODS ON 6 MARCH 1982. (The values below each data set name indicate the number of grid points used in the calculations. Units are in °C.)

TEMPERATURE ALL-TIMES (1-5) RAO-SAT

PRESSURE LEVELS	PHYSICAL MEAN	PHYSICAL STD. DEV.	MODIFIED PHYSICAL MEAN	MODIFIED PHYSICAL STD. DEV.	REGRESSION MEAN	REGRESSION STD. DEV.
100	-2.4	1.1	-0.8	0.9	0.6	0.7
150	-0.2	1.0	1.4	0.8	-0.2	0.7
200	-0.1	1.3	1.3	1.0	1.6	0.9
250	-1.3	1.4	-0.4	1.3	0.4	2.0
300	-1.7	1.6	-1.2	1.4	0.0	1.8
350	-2.2	0.9	-1.6	0.9	-1.6	1.1
400	-1.7	1.4	-1.1	1.5	-1.6	1.4
450	-2.0	1.7	-1.7	2.0	-2.4	1.9
500	-1.7	1.6	-1.4	1.8	-2.4	1.9
550	-1.2	1.3	-0.5	1.3	-1.7	1.5
600	-0.6	1.1	0.5	1.2	-0.6	1.2
650	0.3	1.0	1.8	1.2	0.2	1.1
700	0.4	1.1	2.3	1.4	0.3	0.9
750	0.8	1.1	2.6	1.3	0.9	1.0
800	0.5	1.0	1.7	1.3	0.3	1.3
850	-2.5	1.5	-0.8	1.4	-1.5	1.3
900	-3.8	1.4	-2.9	1.3	-3.2	1.3
SFC	0.7	1.4	0.8	1.4	0.4	1.4

Mean dewpoint differences and standard deviations are presented in Table 3. The moisture biases indicated by the mean differences are quite large for the two physical retrieval schemes but are relatively small for the regression scheme. Both the physical schemes are too moist (warm) in almost the entire lower and middle troposphere with maximum mean dewpoint differences (Rao - Sat < 0) in excess of 6°C at 750 mb. The modified physical scheme indicates a dry (cold) bias of several degrees above 550 mb but the physical does not become dry until 400 mb. The standard deviations of the dewpoint temperature differences for these two schemes range fro 1° to 2°C in the lowest layers up to almost 6°C in the middle troposphere. The regression retrievals indicate only a small dry (cold) bias at the lowest three levels and a slight moist (warm) bias above this. Bias values are less than 2°C at all levels. Despite these small biases, the standard deviations of the dewpoint differences are larger than expected and range from about 2° to 5°C with maximum deviations occurring around 650 and 400 mb. Although these values are not quite as high as for the physical schemes, they indicate a considerable amount of discrepancy from the ground truth data. This will be looked at further in a later section.

TABLE 3. MEAN AND STANDARD DEVIATION OF THE DIFFERENCES BETWEEN THE RAWINSONDE AND SATELLITE GRID POINT TEMPERATURE (DEWPOINT) VALUES FOR A COMPOSITE OF FIVE TIME PERIODS ON 6 MARCH 1982. (The values below each data set name indicate the number of grid points used in the calculations. Units are in °C.)

DEWPOINT TEMPERATURE ALL–TIMES (1–5) RAO– SAT

PRESSURE LEVELS	PHYSICAL		MODIFIED PHYSICAL		REGRESSION	
	MEAN	STD. DEV.	MEAN	STD. DEV.	MEAN	STD. DEV.
100	–	–	–	–	–	–
150	–	–	–	–	–	–
200	–	–	–	–	–	–
250	–	–	–	–	–	–
300	–	–	–	–	–	–
350	–	–	–	–	–	–
400	4.0	3.6	2.7	4.5	1.2	4.8
450	−0.8	4.8	1.3	5.1	−1.0	3.1
500	−2.4	4.6	2.8	5.4	−0.8	2.4
550	−4.4	5.0	−0.6	4.6	−1.4	3.3
600	−3.8	5.4	−1.7	5.2	−0.4	4.3
650	−4.8	5.9	−3.8	5.7	−1.1	4.4
700	−5.9	5.5	−5.9	5.5	−1.5	3.3
750	−6.5	4.8	−6.1	4.3	−1.6	2.4
800	4.0	4.1	−3.4	3.5	0.7	1.7
850	−1.8	2.3	−1.4	2.2	1.4	1.5
900	−1.0	1.4	−0.7	1.4	1.5	1.4
SFC	1.5	2.4	1.4	2.5	1.0	2.3

Geopotential height values calculated from satellite data are derived from the thermal and moisture fields. Any bias patterns reflected in the satellite temperatures should be evident in the height statistics. Warm/cold temperature bias patterns also can cancel out height biases, while on the other hand, constant temperature biases will accumulate (i.e., increase the thickness) and produce increasing height biases with decreasing pressure. Both of these situations occur in the geopotential height data from the VAS satellite soundings on 6 March 1982. Table 4 presents the mean and standard deviation of the differences for the geopotential heights for all five time periods grouped together. As expected, the influence of the temperature biases can be seen in the mean height differences. For the physical retrievals, the low level warm/cold bias pair produce compensating thickness values below 550 mb and result in very little height bias at the middle levels. Above this level, a nearly constant warm bias (Table 2) creates increasingly biased height values which are 60 m too high in the mean at 100 mb. The modified physical

TABLE 4. MEAN AND STANDARD DEVIATION OF THE DIFFERENCES BETWEEN THE RAWINSONDE AND SATELLITE GRID POINT GEOPOTENTIAL HEIGHT VALUES FOR A COMPOSITE OF FIVE TIME PERIODS ON 6 MARCH 1982. (The values below each data set name indicate the number of grid points used in the calculations. Units are in meters).

GEOPOTENTIAL HEIGHT ALL-TIMES (1-5) RAO-SAT

PRESSURE LEVELS	PHYSICAL 638		MODIFIED PHYSICAL 587		REGRESSION 510	
	MEAN	STD. DEV.	MEAN	STD. DEV.	MEAN	STD. DEV.
100	−61.0	27.0	5.6	22.0	−25.0	25.0
150	−44.0	23.0	3.5	23.0	−27.0	27.0
200	−46.0	22.0	−11.5	20.0	−37.0	27.0
250	−42.0	21.0	−14.0	20.0	−44.0	28.0
300	−31.0	21.0	−7.0	23.0	−44.0	31.0
350	−19.0	20.0	1.8	23.0	−37.0	31.0
400	−13.0	18.0	6.3	20.0	−32.0	28.0
450	−6.9	15.0	11.0	17.0	−25.0	23.0
500	−4.8	12.0	17.0	14.0	−17.0	18.0
550	2.4	12.0	20.0	13.0	−11.0	15.0
600	4.6	11.0	20.0	11.0	−8.4	12.0
650	4.9	9.2	17.0	9.3	−7.8	10.0
700	4.2	7.9	13.0	7.5	−8.4	8.6
750	3.0	7.2	8.0	6.6	−9.8	7.8
800	2.1	7.2	3.9	6.6	−11.0	7.1
850	4.3	6.8	3.2	6.6	−10.0	6.4
900	6.5	5.7	8.6	5.8	−5.7	6.1
SFC	−	−	−	−	−	−

retrievals which were extremely cold biased in the 800 to 600 mb layer produced height values that are 20 m too low in the grid mean. This low height bias is not cancelled out until 300 mb where the middle and upper level warm biases greatly increase the thickness values. The regression retrieval mean height difference values are too high (Rao - Sat < 0) for the entire column. This occurs despite some cold biases near 750 mb and 250 mb in the regression retrievals because the warm biases are just too great. Maximum difference values occur in the 300 to 250 mb layer which are less than for the physical scheme but greater than for the modified physical scheme. The standard deviations of the height differences are almost identical for the two physical schemes. Maximum values of just over 20 m occur in the upper levels. Standard deviations for the regression scheme indicate a similar profile but reach 31 m at 350 and 300 mb.

Parameters which represent layer values can be computed and used in order to avoid level biases due to poor vertical resolution in the VAS thermal channels. Tables 5 and 6 present statistical results of all-times combined for thickness calculated over four arbitrary layers of the atmosphere and for precipitable water derived from grid point values of temperature and dewpoint from the surface through 350 mb. Results indicate many of the biases previously discussed (Tables 2 to 4). Mean thickness differences for the four layers (Table 5) vary with each retrieval scheme but correspond to the individual temperature biases. All three of the retrieval sets indicate that thickness is too great in the 500 to 250 mb layer (warm temperature bias) with the physical retrieval scheme being the most biased of -41.0 m. With the exception of the physical retrievals in the upper most layer, the standard deviation of the thickness differences are almost identical from one retrieval scheme to the others. Maximum thickness deviations of around 20 m occur in the 250 to 100 mb layer.

Table 6 presents the mean and standard deviation of the differences for the total precipitable water in the column over the grid region. The physical and modified physical schemes indicate excessive

13

TABLE 5. MEAN AND STANDARD DEVIATION OF THE DIFFERENCES BETWEEN THE RAWINSONDE AND SATELLITE GRID POINT THICKNESS VALUES FOR A COMPOSITE OF FOUR LAYERS OF THE ATMOSPHERE ON 6 MARCH 1982. (The values below each data set name indicate the number of grid points used in the calculations. Units are in meters).

THICKNESS ALL–TIMES (1–5) RAO–SAT

PRESSURE LAYERS	PHYSICAL 638 MEAN	STD. DEV.	MODIFIED PHYSICAL 587 MEAN	STD. DEV.	REGRESSION 510 MEAN	STD. DEV.
100 ↕ 250	–20.0	24.0	20.0	18.0	19.0	17.0
250 ↕ 500	–41.0	16.0	–31.0	15.0	–27.0	16.0
500 ↕ 700	–4.7	9.1	4.2	11.0	–8.5	12.0
700 ↕ 850	–0.1	5.2	9.5	6.9	1.7	5.7

TABLE 6. MEAN AND STANDARD DEVIATION OF THE DIFFERENCES BETWEEN THE RAWINSONDE AND SATELLITE GRID POINT PERCIPITABLE WATER VALUES FOR SURFACE TO 350 mb LAYER OF THE ATMOSPHERE ON 6 MARCH 1982. (The values below each data set name indicate the number of grid points used in the calculations. Units are in millimeters.)

PRECIPITABLE WATER ALL–TIMES (1–5) RAO – SAT

	PHYSICAL 638 MEAN	STD. DEV.	MODIFIED PHYSICAL 587 MEAN	STD. DEV.	REGRESSION 510 MEAN	STD. DEV.
SFC TO 350mb	–1.3	1.8	–0.9	1.4	0.6	0.9

moisture in the precipitable water values while the regression scheme is a little dry biased. This could have been inferred from the dewpoint bias patterns shown in Table 3. Standard deviations are also high for the physical schemes and are around 1.5 mm in this all-time average. The standard deviation of the precipitable water difference for the regression soundings is 0.9 mm for the entire column. The time variability of these bias patterns as well as their cause will be presented next.

B. Statistical Comparison for Individual Times

The statistical results presented in Tables 2 through 6 provide an over-all estimate of the biases and errors in each of the VAS retrieval data sets. These values tend to be smaller than one can expect since the extremes are averaged out in time. The discussion below addresses the VAS thermal and moisture biases graphically as a function of time and of the three retrieval schemes.

Figure 7 presents the mean temperature difference over the grid for each satellite data set as a function of time and pressure. The number of grid points used in the evaluation at each time (occasionally less than the maximum of 130 due to clouds over the grid area) is given below each profile. Several important features are present in Figure 7 which were not apparent in the all-times results (Table 2). First, the low level warm/cold bias couplet is present at most times and has the largest values at the first two time periods. This feature is present in the regression soundings at all-times but turns into a warm bias in the physical and modified physical retrievals for the last two time periods.
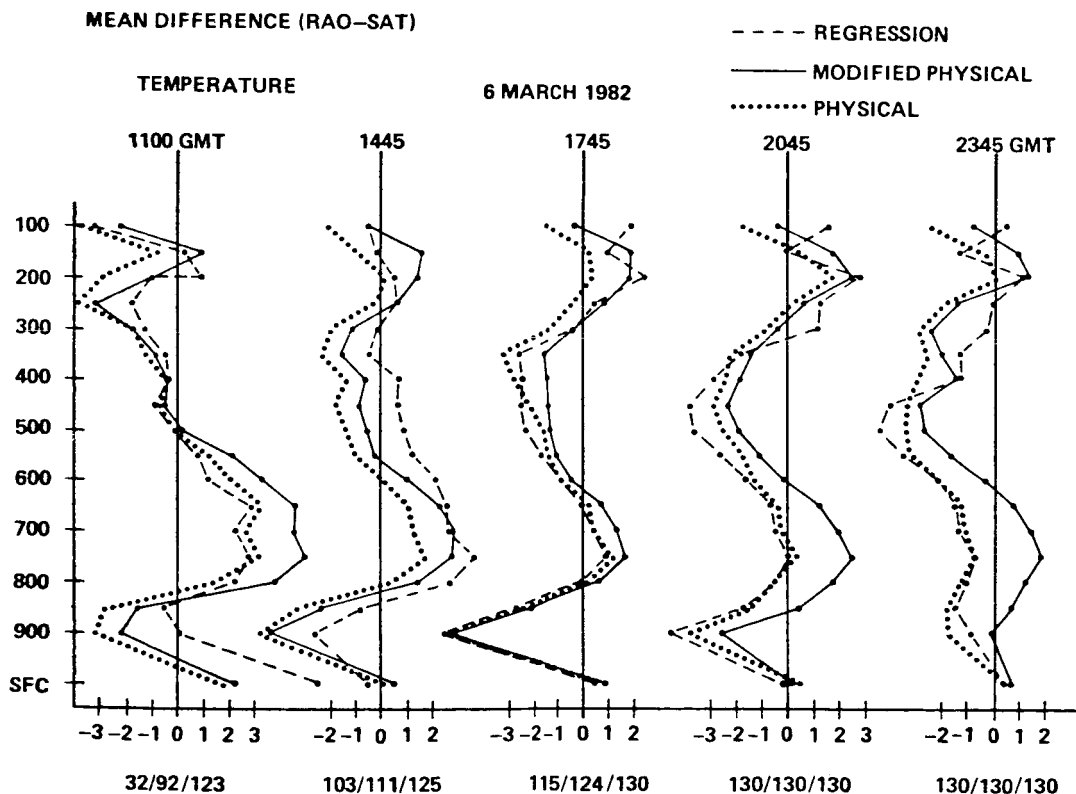

Figure 7. Mean temperature difference between rawinsonde and satellite grid point values as a function of pressure and time. (Dashed lines correspond to regression retrievals, solid lines to the modified physical retrievals, and dotted lines to the physical retrievals. The values below each set of profiles correspond to the number of grid points utilized at each time. All units are in °C.)

Figure 8 presents grid mean profiles of rawinsonde data which indicate the structure of the atmosphere over the grid region. It is readily apparent that the low level temperature bias couplet is due to the strong frontal inversion in the 900 to 700 mb layer. This inversion weakens with time as high pressure moves over the region (Fig. 3a and 3d) and as insolation warms the boundary layer. The smaller biases in the VAS low level temperatures at 2045 and 2345 GMT seem related to the weaking of this inversion. Another feature in the grid mean temperature profiles offers an explanation for the bias patterns in the middle and upper layers. The tropopause inversion present at 1100 GMT (Fig. 8a)
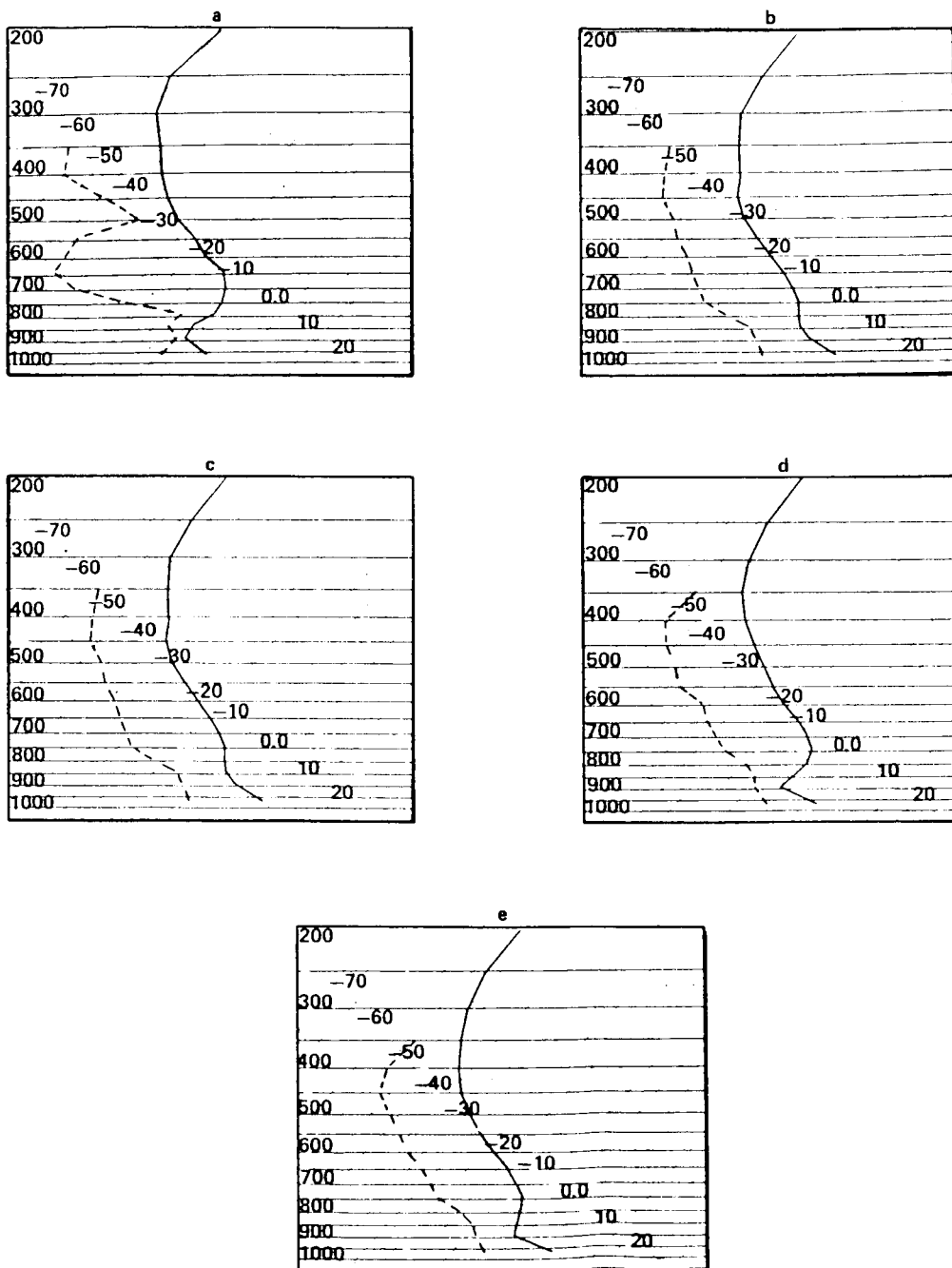

Figure 8. Grid mean temperature and dewpoint profiles (on skew T-log P diagram) for the rawinsonde data at (1) 1100 GMT, (b) 1445 GMT, (c) 1745 GMT, (d) 2045 GMT, and (e) 2345 GMT 6 March 1982.

16

around 250 mb lowers onto the frontal boundary with time and creates a fairly strong inversion in the middle troposphere by 1745 GMT (Fig. 8c). This feature combined with the poor vertical resolution of the middle and upper troposphere VAS channels (Fig. 1) and the low signal-to-noise ratio in these channels seem to prevent an accurate determination of the inversion level and therefore produce the middle level temperature biases observed in all three retrieval schemes at 1745, 2045, and 2345 GMT. These warm temperature biases are maximized at 2045 GMT with values between 2° and 4°C from 600 through 350 mb. The regression scheme is not biased in this region with a maximum value of 3.9°C at 450 mb. This warm bias is capped by a cold bias (Rao - Sat > 0) above 300 mb at 1745 and 2045 GMT in a similar fashion to the low level bias couplet.

Figure 9 presents the mean dewpoint temperature differences as a function of time and retrieval scheme over the mesoscale grid region. The difference profiles exhibit many of the biases noted in the all-times results (Table 3) but also indicate some diurnal variation. The physical and modified physical schemes have a moist (warm) bias (Rao - Sat < 0) through most of the column between 1100 and 1745 GMT. Maximum difference values for these schemes exceed 8°C around 700 mb. The physical schemes become slightly less biased in the lowest layers at 2045 and 2345 GMT but become dry (cold) biased above 600 mb at these times. Maximum dry biases exceed 5°C in the 450 to 350 mb layer. Except for the very large moist (warm) bias at 1100 GMT, the regression retrievals exhibit only minor dewpoint temperature biases at all times. The large bias in the 750 to 550 mb layer at the first time may be due to the relatively few data points used in the calculation due to cloud cover, however, similar biases exist for the two physical schemes with a larger number of grid points. The biases for the regression retrievals are generally less than 3°C but tend to indicate a somewhat larger dry bias in the upper levels. Figure 8 presented the grid mean dewpoint profile (dashed line) from the rawinsonde data for each time indicating the vertical moisture structure over the region. The greatest vertical variation of moisture (dewpoint values) exists at the first time with moist air below 800 mb and in a thin layer from 550 to 400 mb. This corresponds to the large bias area previously discussed. An extremely dry layer of air exists between these moist layers. At the later times, the grid mean dewpoint profiles become less variable and the satellite biases become somewhat less. The vertical structure revealed by the satellite soundings will be discussed in the next section.
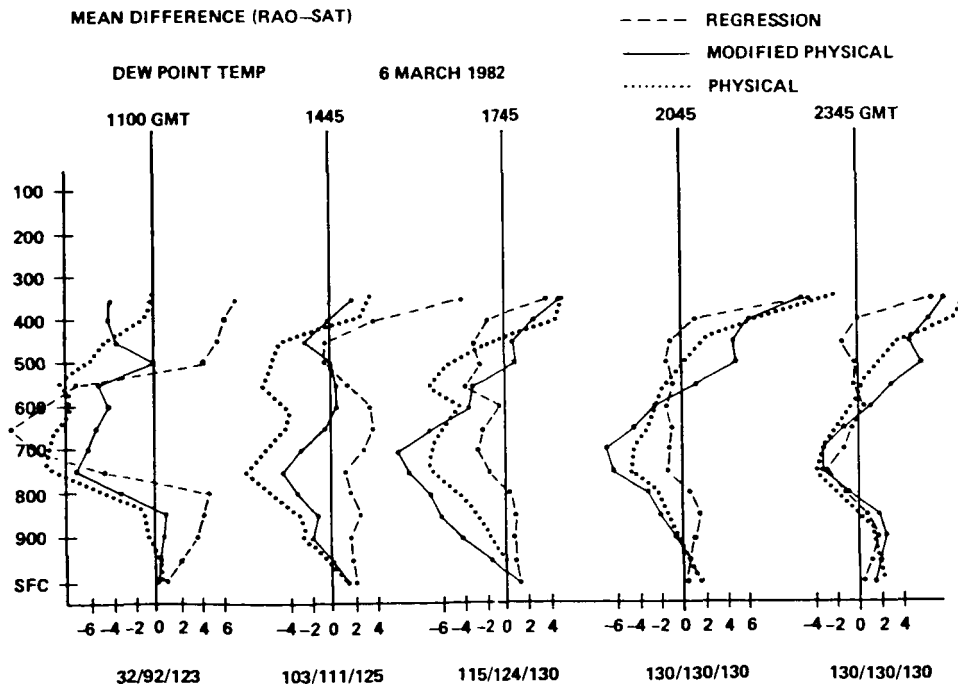

Figure 9. Same as Figure 7 except for dewpoint temperature.

The time variability of the geopotential height biases are presented in Figure 10. These height biases correspond directly to the temperature biases indicated in Figure 7. The warm temperature biases which are prevalent in the middle troposphere after 1745 GMT produce considerably large height biases above 500 mb. This was only vaguely apparent in the all-times average in Table 4. Magnitudes of the height biases exceed 60 m at 300 mb for the regression scheme from 1745 through 2345 GMT. The upper level height biases for the physical scheme range from 40 to 60 m at all times while the largest biases for the modified physical scheme reach nearly 40 m only at the last time. In the lowest layers, there is a tendency in both of the physical retrieval sets to change from a negative height bias to a positive one with time. This seems most definitely related to the decay of the low level frontal inversion shown in Figure 8.
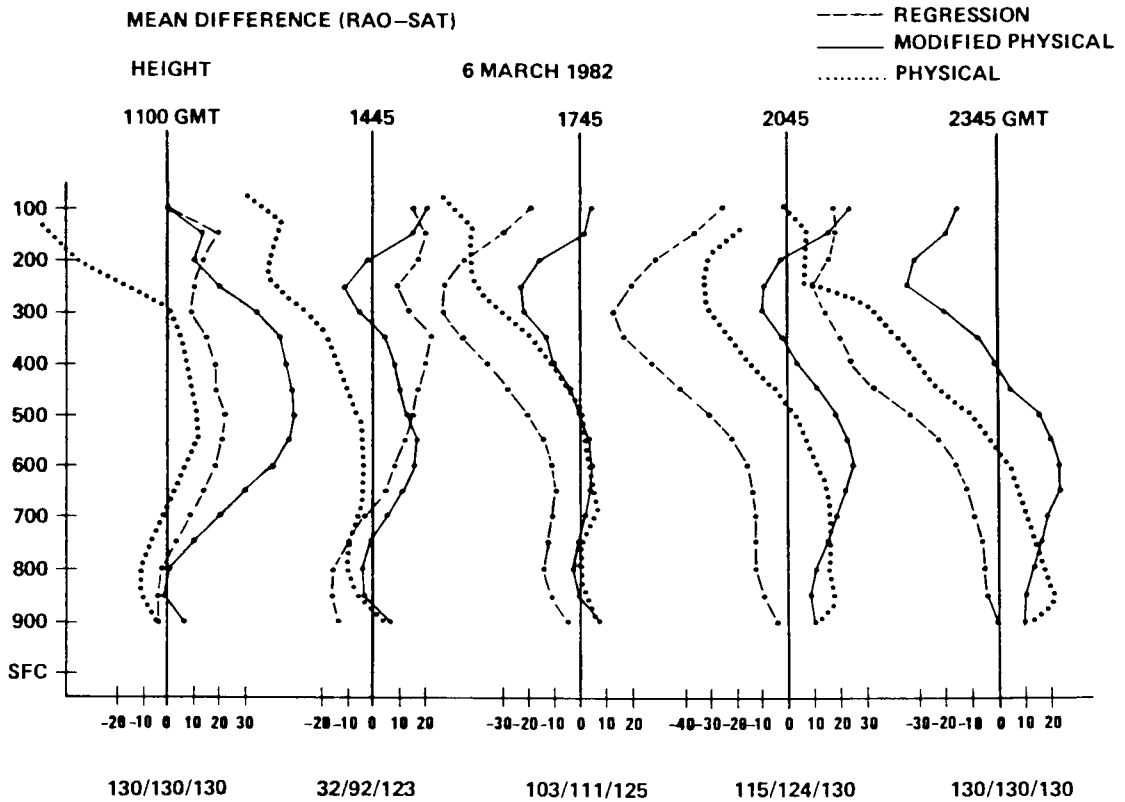
Figure 10. Same as Figure 7 except for geopotential height (units are in meters).

The time variability of the precipitable water differences are shown in Figure 11 for the three retrieval schemes. The physical and modified physical schemes indicate a major moist bias at most times with values approaching 3.0 mm at 1445 and 1745 GMT, respectively. This bias is reduced to a negligible dry bias at 2345 GMT. Although 3.0 mm does not seem like a lot, it represents roughly a 30 percent error when the total precipitable water amount of 10.0 mm is considered. The regression soundings are only slightly biased at the first two times and compare well with the precipitable water determined with the ground truth data from 1745 GMT through 2345 GMT. This similarity was also indicated in the dewpoint results.

Figure 11. Mean precipitable water differences between the rawinsonde and satellite grid point values as a function of time. (Dashed lines correspond to regression retrievals, solid lines to modified physical retrievals, and dotted lines to physical retrievals. All units are in millimeters.)

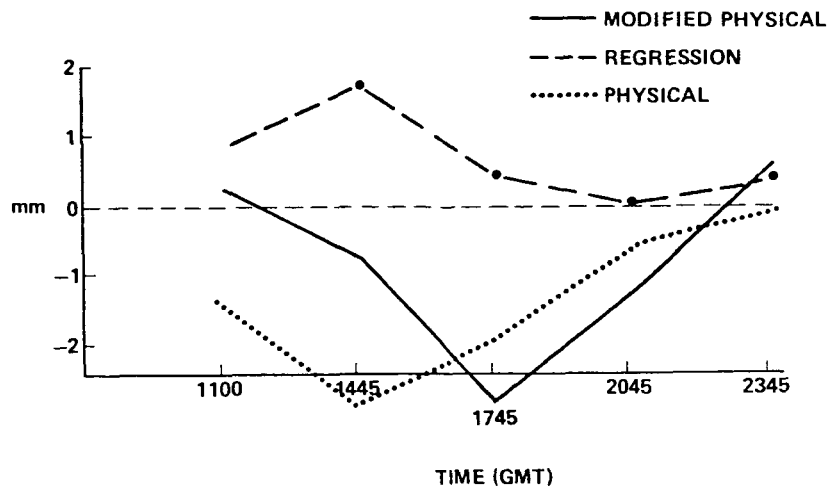## C. Vertical Structure Depicted by VAS Sounding Data

The vertical variation of the temperature and moisture biases discussed above indirectly evaluated the vertical resolution of the VAS sounding data sets. Figure 12 presents the grid mean profiles of the rawinsonde and satellite data sets at 1745 and 2345 GMT in order to directly compare the vertical structure resolved by the VAS soundings at these times. Grid point values for the entire cloud-free grid region were averaged to produce these vertical profiles. At 1745 GMT (Fig. 12a-c), the structure of the atmosphere, as determined by the grid mean rawinsonde profile (solid lines), indicates the presence of a strong frontal inversion extending from about 900 through 750 mb over the grid region. Below 900 mb the boundary layer is gradually being warmed by solar heating. The dewpoint profile indicates significant drying above the frontal inversion with dewpoint depressions greater than 15°C up to 350 mb (where the profile indicates an increase in moisture). The physical retrieval grid mean profile (Fig. 12a, dot-dashed line), indicates a very smooth temperature and moisture profile. The frontal inversion in almost completely smoothed out. The tropopause inversion around 350 mb is also not well captured by the physical retrievals. From this diagram, it would be difficult to determine the level of the frontal inversion from the satellite profile alone. The tropopause, as determined by the physical retrievals is misplaced by at least 100 mb. The temperature and moisture biases previously discussed are also apparent. It is important to note that the dewpoint depression is almost half that of the rawinsonde between 850 and 400 mb.

The grid mean vertical profile for the modified physical soundings (Fig. 12b, dashed line) does not describe the vertical structure of the atmosphere any better than the physical soundings. The temperature profile is similar, but the dewpoint profiles is much more moise biased at this time (as previously noted). Thus the dewpoint profile does not come close to portraying an accurate vertical structure. The grid mean profile for the regression retrievals at this time (Fig. 12c, dotted line) presents a similar

19
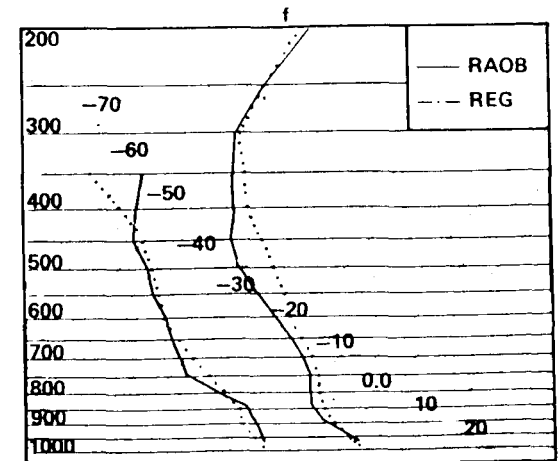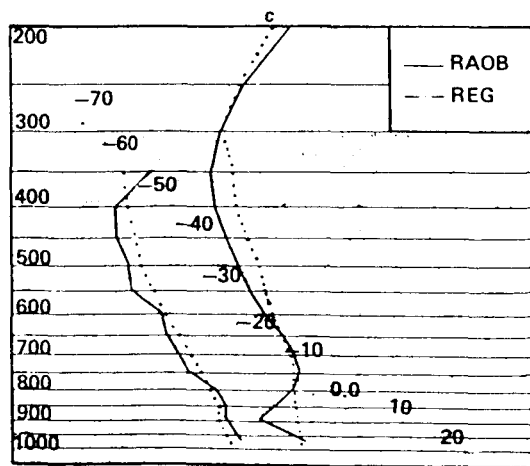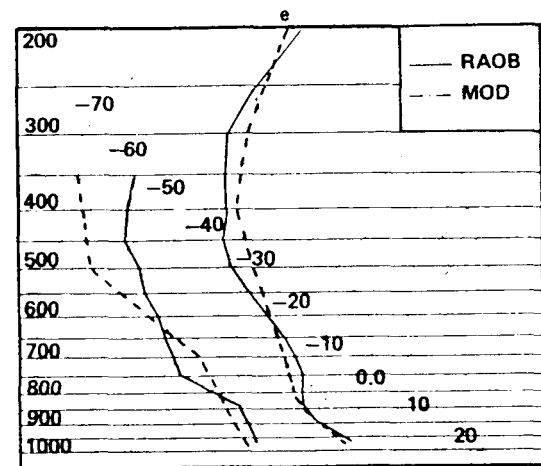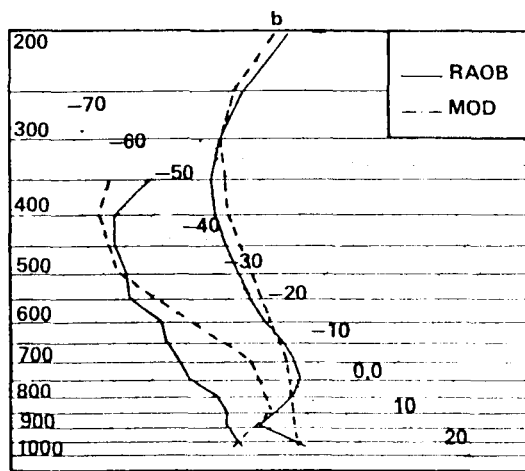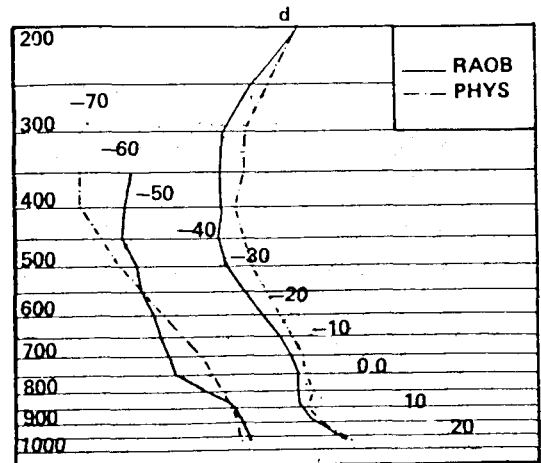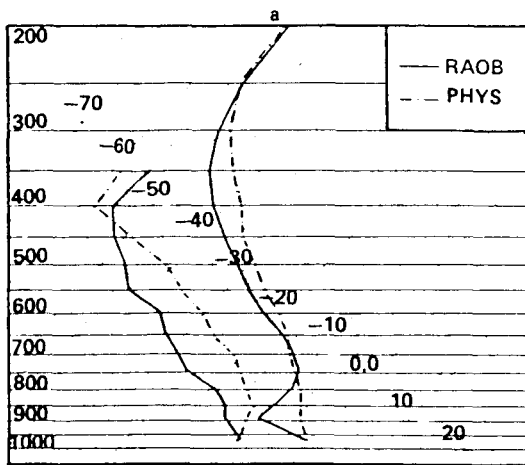
Figure 12. Grid mean profiles (skew T-log P) of temperature and dewpoint temperature at 1745 GMT for the (a) physical, (b) modified physical, and (c) regression retrievals. Similar profiles at 2345 GMT are presented in (d), (e), and (f) for the three retrieval schemes, respectively. The solid line in each figure corresponds to the rawinsonde grid mean profile shown in Fig. 8c and 8e.

problem with the temperature structure but shows a substantial improvement over both of the physical retrieval sets in determining the vertical moisture structure. The regression dewpoint profile is within several degrees of that of the rawinsonde at all levels and portrays the lapse rate of dewpoint quite well. It should be noted that the rawinsonde dewpoint contains no significant change in lapse rate from the surface to 400 mb and therefore should be less difficult to represent.

At 2345 GMT (Fig. 12d-f), the rawinsonde grid mean profile indicates an ill-defined frontal inversion and a weaker and less well defined middle and upper troposphere inversion than at 1745 GMT. The moisture profile is beginning to show a little more of a subsidence inversion with a rapid drying out above 850 mb. The physical retrieval grid mean temperature profile (Fig. 12d) defines the vertical temperature structure of the atmosphere somewhat better than it did at 1745 GMT. This is undoubtably due to the lack of strong inversions at this time. The physical retrievals keep an almost constant dewpoint depression with height however, and do not capture the dry air aloft very well. The modified physical retrievals (Fig. 12e) present a little different picture than the physical ones. While the temperature profile is different, it does not show any major improvement over the physical one, but just indicates a different type of bias. There is only a slight hint of the lowered tropopause inversion at 400 mb. The dewpoint profile for the modified physical scheme indicates substantial vertical structure but does not correspond well to the rawinsonde grid mean profile. The regression retrievals at 2345 GMT (Fig. 12f) do a reasonably good job of describing the vertical temperature and moisture structure. The major inversion at the tropopause is portrayed well at 300 mb, however, the lessening of the temperature lapse rate in the 500 to 400 mb layer is missed. The dewpoint profile again does a good job of representing the moisture structure. The almost constant lapse rate of dewpoint temperature lacks the drying out due to subsidence as indicated in the rawinsonde profile, however.

D. Horizontal Structure

It is believed that VAS is capable of determining fine mesoscale horizontal structure in the atmosphere because of its small spatial field of view and only limited horizontal averaging is needed to increase the signal-to-noise ratio to a tolerable level. A measure of this horizontal structure is indicated in gradient information of the various parameters. Table 7 presents the mean and standard deviation of the differences between the satellite and rawinsonde temperature gradients (magnitude) calculated over the mesoscale grid region. The number of grid points over which the statistics are calculated is reduced due to the centered finite differencing technique. In the all-times average, the satellite temperature gradients are somewhat weaker than those of the rawinsonde (Rao - Sat > 0). Maximum differences appear around 500 mb with values of 1.0 to 1.3°C/100 km. For typical mesoscale features of 400 to 600 km this can be quite significant. Values in the lower and upper levels are considerably reduced providing a better estimate of the actual temperature gradient. None of the retrievals indicate that they represent the temperature gradients better than the other in the grid mean. Negative mean difference values occur at several levels which indicate that the satellite temperature gradient is stronger than that of the rawinsonde. At first this situation is a little difficult to understand, but several explanations are possible. It is doubtful that over the relatively large mesoscale domain of the analysis region that the true atmospheric gradient is actually much stronger than that of the rawinsonde. This might be true at very small scales (below that resolvable by the rawinsonde) but not over the grid region. Vertical and horizontal aliasing by VAS may explain tighter than normal gradients over a given region. Also, stronger gradients may appear where the rawinsonde gradients are relatively small. Standard deviations of the gradient differences also indicate largest variations in the 500 to 300 mb layer where values exceed 1.0°C/100 km. This trend is almost identical for each VAS data set.

Figure 13 presents an example of the horizontal structure derived from VAS radiance data for 500 mb temperature at 2345 GMT. The rawinsonde data (Fig. 13a) indicate a cold pocket situated over

21

TABLE 7. SAME AS TABLE 2 EXCEPT FOR THE MAGNITUDE OF THE TEMPERATURE GRADIENT. (Units are in °C/100 km.)

MAGNITUDE TEMPERATURE GRADIENT ALL −TIMES (1−5) RAO−SAT

| PRESSURE LEVELS	PHYSICAL 433 MEAN	PHYSICAL 433 STD. DEV.	MODIFIED PHYSICAL 390 MEAN	MODIFIED PHYSICAL 390 STD. DEV.	REGRESSION 329 MEAN	REGRESSION 329 STD. DEV.
100	0.0	0.8	0.4	0.7	0.2	0.6
150	−0.1	0.7	0.2	0.7	0.3	0.6
200	0.3	0.9	0.5	0.8	0.3	0.8
250	0.7	0.9	0.9	0.8	0.1	1.0
300	0.1	1.0	0.3	1.0	0.3	1.2
350	−0.1	0.9	0.1	0.8	−0.3	1.0
400	0.4	1.3	0.7	1.2	0.5	1.4
450	1.0	1.2	1.3	1.2	1.2	1.4
500	0.8	1.1	1.2	1.1	1.0	1.1
550	0.5	1.1	0.8	0.9	0.7	0.9
600	0.3	0.8	0.3	0.8	0.2	0.7
650	0.2	0.7	0.2	0.7	0.1	0.7
700	0.2	0.8	0.1	0.9	0.1	0.9
750	0.3	0.9	0.3	0.9	0.3	0.8
800	0.3	0.9	0.3	0.9	0.4	0.7
850	0.2	1.0	0.1	1.0	−0.1	0.8
900	0.3	0.7	0.3	0.7	0.0	0.9
SFC	0.7	0.8	0.7	0.8	0.9	1.6
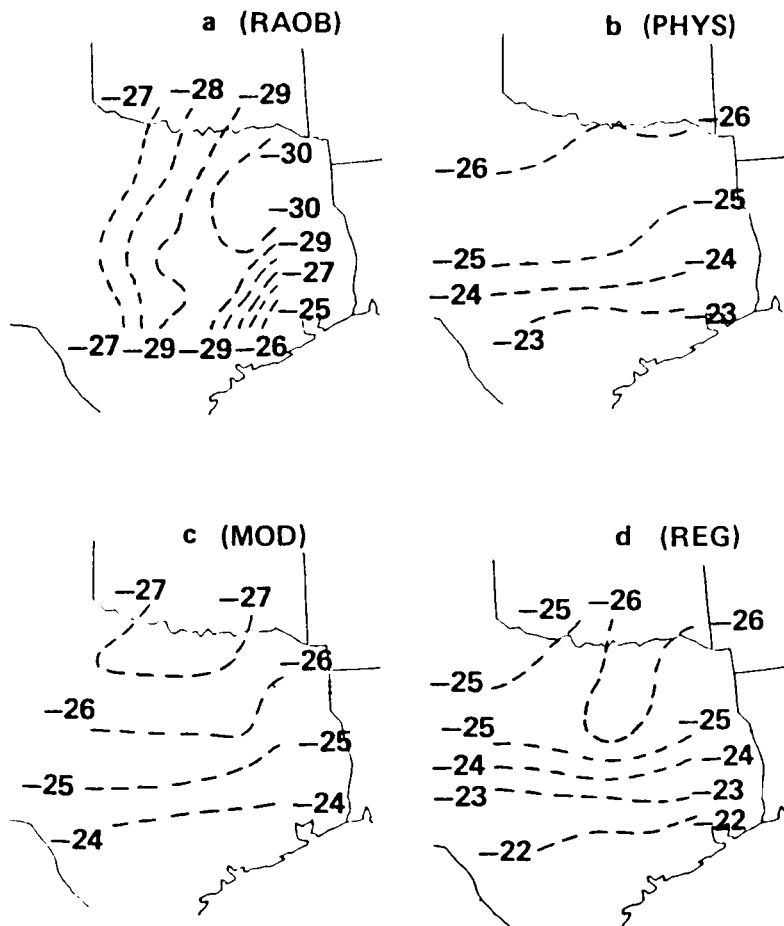
Figure 13. Horizontal analysis of temperature at 500 mb for 2345 GMT for the (a) rawinsonde, (b) physical, (c) modified physical, and (d) regression soundings (all units are in °C).

the northcentral portion of the mesoscale region. A strong gradient exists around this cold area with a west-east orientation on the west side and a somewhat tighter gradient to the southeast. The physical retrievals (Fig. 13b) present a rather bland temperature gradient with a north-south orientation. This is quite a bit weaker than the rawinsonde and fails to capture the cold pocket over the network. The modified physical retrievals (Fig. 13c) show a similar weakened gradient but indicate a cold pocket in the northern part of the region. The regression retrievals (Fig. 13d) capture the cold pocket fairly well and center it near the actual rawinsonde location. The gradient around this is somewhat stronger than the two physical retrieval sets but is still orientated in the north-south direction. None of the schemes capture the reversal of the temperature gradient to the west of the cold region very well. A warm bias across most of the region is also apparent in the fields as was pointed out in previous sections.

Table 8 presents the mean and standard deviation of the differences between the rawinsonde and satellite dewpoint temperature gradients (magnitude) in the all-time average for each retrieval scheme. In general, all three retrieval schemes indicate reduced dewpoint gradients over the mesoscale region with maximum values reaching just greater than 3.0°C/100 km at 600 and 650 mb. There are a few levels where the satellite gradients are stronger than the rawinsonde and the explanations used above are also applicable here. Standard dewpoint gradient deviations range from about 1.0°C/100 km in the lower levels to 3.3 around 550 mb. The regression values are somewhat larger than for the two physical data sets indicating more uncertainty in this horizontal measurement. This is important since the regression retrievals produced the least biased moisture results in the grid mean. From this further evaluation, it seems that the regression soundings represent the mean moisture distribution quite well but do not provide detailed mesoscale variability.

TABLE 8. SAME AS TABLE 2 EXCEPT FOR THE MAGNITUDE OF THE DEW-POINT TEMPERATURE GRADIENT. (Units are in °C/100 km.)

MAGNITUDE DEWPOINT TEMPERATURE GRADIENT ALL-TIMES (1-5) RAO-SAT

PRESSURE LEVELS	PHYSICAL 433 MEAN	STD. DEV.	MODIFIED PHYSICAL 396 MEAN	STD. DEV.	REGRESSION 329 MEAN	STD. DEV.
100	–	–	–	–	–	–
150	–	–	–	–	–	–
200	–	–	–	–	–	–
250	–	–	–	–	–	–
300	–	–	–	–	–	–
350	–	, –	–	–	–	–
400	1.5	3.0	0.8	2.4	-0.4	4.0
450	0.7	3.2	-0.4	2.9	0.1	2.3
500	0.9	3.4	-0.3	3.3	1.6	2.6
550	1.8	3.5	1.5	3.3	2.1	3.9
600	2.8	3.6	3.2	3.1	3.1	4.5
650	3.0	3.7	3.1	3.2	3.2	4.6
700	2.5	3.3	1.9	3.0	2.6	3.6
750	2.1	3.2	1.6	3.1	1.9	2.8
800	0.6	2.0	0.1	2.0	0.5	1.5
850	-0.1	1.5	-0.4	1.4	0.0	1.3
900	0.1	1.1	-0.1	1.0	0.2	1.0
SFC	1.3	1.9	1.3	1.8	0.9	2.2

Figure 14 evaluates the direction portion of the gradient for dewpoint at 700 mb and 2345 GMT. The rawinsonde data indicates a dry region in the northern portion of the analysis area with an appendage stretching down to the southeast. Increasing moisture (warmer temperatures) exist with a tighter gradient to the south. None of the VAS retrieval analyses does an extremely accurate job of portraying this quantity, however, the modified physical retrievals do the best. The dry region is captured fairly well by the modified physical retrievals with the increasing dewpoint gradient to the south. The only questionable area is in the extreme northwestern portion of the region. The physical and regression retrievals do about an equally poor job at defining the dewpoint structure. Both present a dry region centered over the network with only weak gradients surrounding it. Despite the lack of detailed mesoscale agreement, these data sets do present a smoother version of the rawinsonde dewpoint field and may provide significantly useful information at a somewhat larger scale.
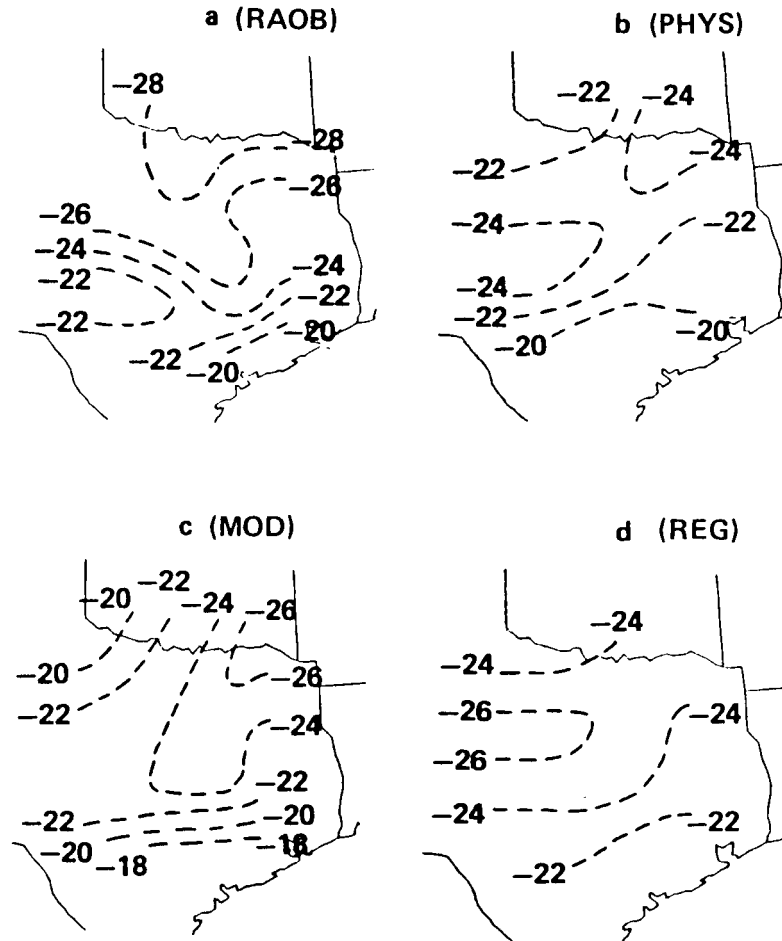
Figure 14. Same as Figure 13 except for dewpoint temperature at 700 mb.

E. Apriori Information

The application of remote sensing instruments to the retrieval of temperature and moisture profile information necessitates inverting the radiative transfer equation. The solutions can take many forms, but in each case some apriori information is needed about the atmosphere. This information must consist of an atmospheric model (with thermal and moisture characteristics) from which the transmission of radiation through the atmosphere can be calculated. Physical retrieval schemes like the two evaluated in

this paper use an iterative process to improve on a first guess temperature and moisture profile. Any temperature and moisture profile can be used, however, a profile of the atmosphere which is representative of the actual sounding environment produces the best retrieved soundings. The procedure used to produce the regression soundings in this study also uses apriori temperature and moisture information but in a somewhat different manner. These profiles are used along with co-located radiance measurements to develop relationships between the two data types. These relationships are then applied to other radiance measurements. Chesters, et al. [3] have indicated that sounding results are best when local soundings (those having structural features similar to the sounding environment) are used to develop the regression matrix.

The first guess information used in the two physical retrieval schemes was the initial and 12 hr forecast fields from the operational Limited Fine Mesh (LFM) numerical model run at the National Meteorological Center. For the five time periods at which retrievals were made on 6 March 1982, temperature and moisture profiles were derived from the LFM grid point data. At 1100 and 2345 GMT, the initial and 12 hr forecast fields were used, respectively. For the three in-between times, a linear interpolation to the sounding time was used from the initial and 12 hr forecast. For the regression retrievals, NWS rawinsonde data were used at 1200 GMT 6 March and 0000 GMT 7 March. These data were not those available operationally, but from the special AVE/VAS experiment conducted on those days. (Only the NWS soundings and not the special site soundings were used.) This data is derived differently, producing 40 levels of data at 25 mb increments from typically 140 to 170 contact data points and provides better vertical resolution than those produced operationally.

In order to evaluate the structural content of the first guess LFM data, the data were bi-linearly interpolated to the mesoscale grid used for the satellite and rawinsonde data and presented in Figure 2. The gridded LFM data then were evaluated in a similar fashion to the satellite data and mean and standard deviations of the differences between the rawinsonde and the LFM first guess data were calculated and are presented in Table 9 for temperature and dewpoint. In the all-times average, the LFM first guess data shows some of the same temperature and moisture biases as do the physical and modified physical retrievals. A low level temperature bias couplet is present below 700 mb with a magnitude which is intermediate to the two physical retrieval data sets. A small warm bias (Rao - LFM < 0) is present at 500 mb. The warm bias in the satellite retrievals was previously shown to be somewhat stronger at this level (Table 2) and extended over a deeper layer. The first guess data indicates a strong cold bias in the upper most levels in the all-times average with magnitudes exceeding 3°C at several levels. This is similar to the modified physical retrievals which show the same trend. The physical retrievals show a tendency towards a cold bias at these levels but remain slightly warm biased in this area. The standard temperature difference deviations for the first guess data are nearly identical to those of the physical and modified physical retrievals ranging from about 1° to 2°C with a maximum in the middle and upper levels.

The mean dewpoint difference between the rawinsonde and the first guess LFM data (Table 9) indicates that in the all-times average the first guess data was moist biased in the lower levels and dry biased aloft. This pattern is similar to the two physical schemes, however, the dry bias is slightly greater in the LFM data. Standard deviations are also comparable. These biases are not surprising since some vertical smoothing of the input (rawinsonde) data is performed in the interpolation to the LFM levels during model initialization. It is surprising that (in the all-times average) little if any improvement in the vertical structure of the atmosphere is made with VAS.

Figure 15 shows the grid mean LFM guess profile at 1745 GMT which can be compared to those of the physical retrieval data sets in Figure 12a and b. As indicated in the all-times results, similar biases exist in the LFM and satellite sounding data as shown here at 1745 GMT. The issue of importance is whether the satellite soundings have improved vertical resolution over the first guess information. In the temperature profiles, the VAS temperature curves are shifted slightly resulting in a magnitude difference

25

TABLE 9. MEAN AND STANDARD DEVIATION OF THE TEMPERATURE AND DEWPOINT TEMPERATURE DIFFERENCES BETWEEN THE RAWINSONDE AND LFM FIRST GUESS GRID POINT DATA FOR A COMPOSITE OF FIVE TIME PERIODS ON 6 MARCH 1982. (Units are in °C.)

LFM GUESS   ALL TIMES (1–5) RAO–LFM

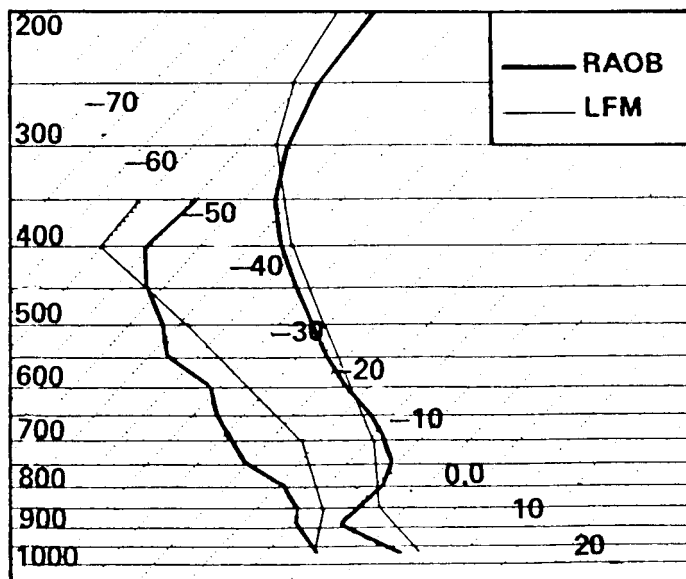|		T 650		TD 650	
		MEAN	STD. DEV.	MEAN	STD. DEV.
	100	0.65	0.92	—	—
	150	3.30	0.83	—	—
	200	3.20	1.20	—	—
	250	1.70	1.50	—	—
	300	1.10	1.60	—	—
PRESSURE LEVELS	400	0.43	1.40	6.6	4.4
	500	−0.75	1.90	0.3	4.1
	700	1.90	0.92	−5.3	6.0
	850	−0.77	1.30	−1.4	1.6

Figure 15. Grid mean profile (skew T- log P) of temperature and dewpoint for the LFM first guess information at 1745 GMT (thin line). (The rawinsonde grid mean profile is presented by the bold line. VAS profiles for this time are shown in Figure 12.)

in the bias pattern. It is not apparent that any significant improvement is made over that of the first guess information at this time period. Above 300 mb, there seems to be some improvement over the first guess, mainly in the physical retrievals (Fig. 12a). This improvement, however, seems to be at the expense of a larger bias in the middle layers. A vertical profile of the grid mean dewpoint values from the first guess information at 1745 GMT is also presented in Figure 15. Figures 12a and b can be used to compare the vertical moisture structure of the satellite data. The LFM and the physical retrieval dewpoints are almost equivalent while the modified scheme tends to be moister in the lower levels and slightly drier aloft. These results tend to indicate that in the average, very little improvement in the vertical resolution is made by either physical retrieval scheme over that of the first guess information.

The horizontal structure defined by the LFM first guess information should be relatively bland at the mesoscale because of the large scale information utilized by the model and a relatively course grid spacing. Figures 16 and 17 present a horizontal analysis of some of the first guess information over the mesoscale grid region. The 500 mb temperature field (Fig. 16) shows only a weak north-south gradient over the region. This figure can be compared to Figure 13 which presents the 500 mb analyses from the rawinsonde and the VAS retrieval data sets. The first guess temperature field does not represent that of the rawinsonde at all. There is significantly more variability at the mesoscale. The retrieved VAS soundings from the physical and modified physical schemes improve over the first guess information by increasing the temperature gradient across the network. However, the direction of the gradient in the VAS retrievals remain more like the first guess than the rawinsonde. This could be due to a dependence of both physical retrieval schemes on the first guess information [5]. The LFM first guess information for dewpoint at 700 mb on 2345 GMT 6 March (Fig. 17) presents a somewhat different situation. The structure to the LFM dewpoint gradient is significant with a fairly strong gradient over the network. This is somewhat in agreement with the rawinsonde analysis (Fig. 14a) but shows some discrepancy in the northern half of the region. The VAS sounding analysis for dewpoint at this level and time (Figs. 14b and 14c) indicate some similarities to the first guess but also some distinctively different structure some of which correlates well with that of the rawinsonde as discussed in the previous section.
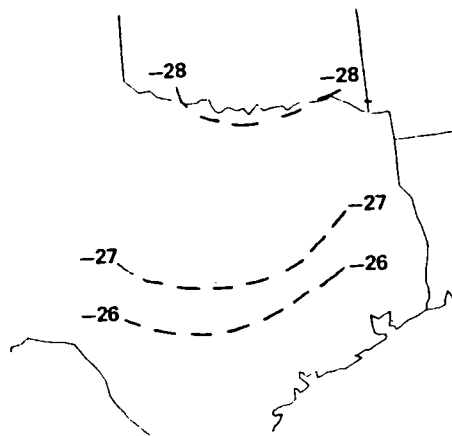

Figure 16. LFM first guess analysis of 500 mb temperature at 2345 GMT
6 March 1982 interpolated to the mesoscale grid. (Units are in °C.)
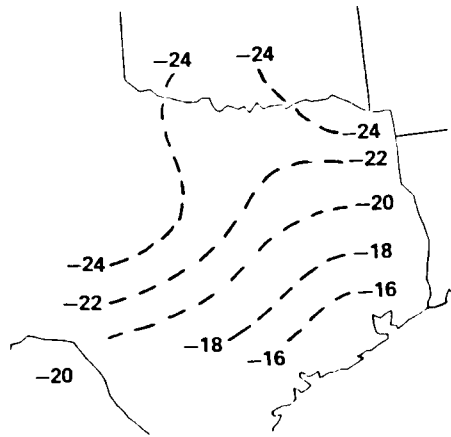
27

Figure 17. Same as Figure 16 except for 700 mb dewpoint values.

It is difficult to evaluate the dependence of the regression retrievals on the first guess information because the scheme does not directly use this information in a manner similar to that of the physical schemes. The available information used by the regression scheme contains significantly more vertical structure than the LFM first guess profiles. Presumably, much of the vertical structure of the atmosphere over the grid region is lost or hidden by the coarse vertical resolution of the VAS channels (Fig. 1). The retrieval algorithms may further reduce this structure and thereby present soundings of the quality presented in this paper. It would seem that improved vertical resolution in satellite sounding data, above what has been presented here, lies with an instrument having more channels which better delineate the layers of the atmosphere from which radiation is emitted.

VI. DATA DISCREPANCIES AND ERROR BOUNDS

A. Rawinsonde Errors

The findings presented in the results section were based on the assumption that the rawinsonde data accurately portray the "real" mesoscale structure of the atmosphere. For the most part, this assumption is valid since radiosonde data are conventional measurements with proven reliability and are used almost exclusively in atmospheric research. This special experiment data set was also the subject of rigorous data checks during the reduction process [13]. However, instrument error is a factor which has not been considered so far and may provide some further explanation for the rawinsonde-satellite discrepancies. Figure 18 presents the maximum RMS error expected of the rawinsonde data as a function of pressure based on the study by Fuelberg [15]. These errors are based solely on instrument constraints. Also presented are the RMS errors for all three retrieval sets presented above based on the all-times RMS difference between the rawinsonde and VAS sounding data. The RMS temperature error for the rawinsonde is $0.5°C$ at all levels (Fig. 18a). This is substantially smaller than that of each retrieval scheme in which values range from $2°$ to $3°C$ at most levels.

Figure 18b presents the same comparison for dewpoint temperature. In this case, a rawinsonde RMS relative humidity error of 10 percent translates into a varying dewpoint error for the rawinsonde. In the cold, dry, middle troposphere, the RMS errors become greater than $4°C$, however, the RMS errors for the physical and modify physical retrievals still exceed this value by several degrees. The regression RMS errors are similar to those of the rawinsonde except above 450 mb where they greatly exceed the rawinsonde error values. This is consistent with the comparisons in the previous section which indicate that the dewpoints from the regression retrievals are quite good in the mean but suffer slightly in horizontal detail.
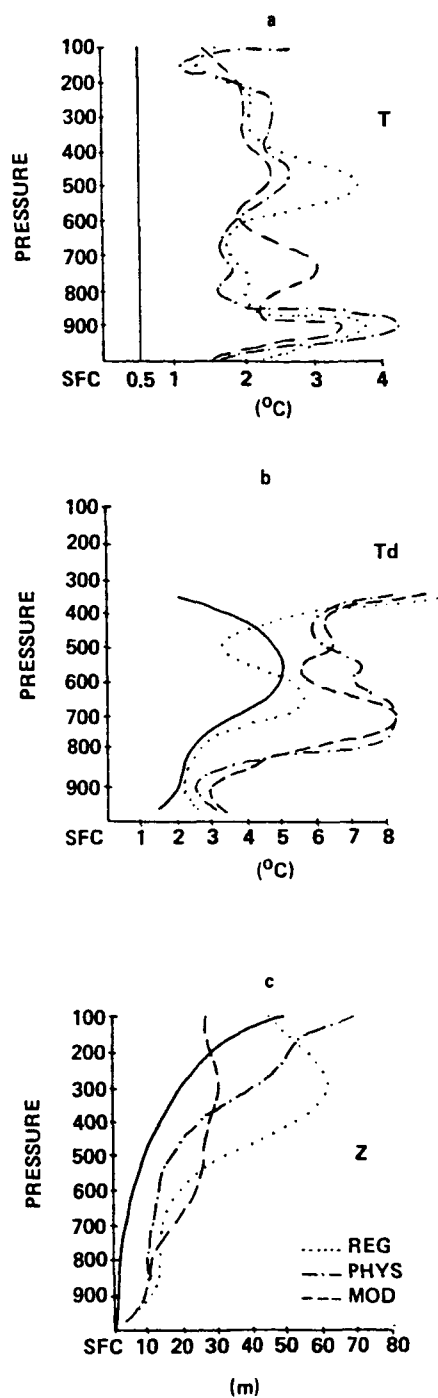
28

Figure 18. Root-Mean-Square (RMS) errors for rawinsonde data as a function of pressure [15] and RMS differences between grid point values of rawinsonde and satellite data for an all-times average for (a) temperature, (b) dewpoint temperature, and (c) geopotential height for each satellite retrieval scheme. Dotted lines indicate the regression results, dot-dashed for the physical, and dashed lines for the modified physical retrieval results. Units are in °C for the temperature and dewpoint curves, and in meters for the height curves.

The RMS error for geopotential height (Fig. 18c) calculated with assumed rawinsonde temperature errors (Fig. 18a) becomes increasingly larger as the temperature errors accumulate. These errors are still relatively small however, reaching 10, 20, and 50 m at 500, 300, and 100 mb, respectively. The VAS RMS errors for all-times are considerably larger than those of the rawinsonde at all levels except the uppermost ones. Maximum differences occur in the middle and upper levels. These results tend to indicate the rawinsonde errors for the most part contribute little to the observed temperature discrepancies of the rawinsonde-satellite comparisons. For dewpoint temperature, the rawinsonde errors may be nearly as large as the rawinsonde-satellite discrepancies especially in the middle troposphere. The results for geopotential height indicate that below 300 mb rawinsonde height errors are small compared to those of the satellite. Above this level, the rawinsonde height errors may account for some of the differences between the two data types.

B. Satellite Radiance Errors

Other contributing factors in the rawinsonde-satellite discrepancies can be due to the accuracy of the radiometer making the remote measurements. For VAS, errors in the radiance measurements can be quite large, however, with multiple spins and spatial averaging, this error is reduced to less than 0.5eK in each channel. The effects of this error reduces vertical resolving capabilities of the instrument and degrades the vertical resolution in the retrieved profiles. Other factors, such as clouds, can contaminate what seem to be clear fields of view and therefore bias a particular radiance measurement. Although manual and automated techniques are used in the retrieval process to eliminate cloudy radiance measurements (Smith [5]; Lee, et al. [4]), small scale cloud features (less than 15 km in diameter) can often go undetected. These measurement problems are very difficult to handle but do affect the accuracy of the retrieved soundings.

C. Sampling Problems

One of the major factors affecting rawinsonde-satellite comparisons is the difference in the type of measurement obtained with each instrument. The rawinsonde values are virtually point measurements of quantities which vary greatly in space. This is especially true for rawinsonde moisture measurements which often exhibit significant moisture variations over thin layers of the atmosphere and at small horizontal distances. The satellite temperature and moisture profiles are derived from radiance measurements which originate from thick layers of the atmosphere and relatively large horizontal extents (Fig. 1). A satellite radiance measurement (single field of view) is actually a volumetric average from a slab of the atmosphere. This problem has been addressed by Bruce et al. [16] who found that this sampling problem can often account for several degrees of discrepancy between the rawinsonde and satellite measurements. The VAS retrievals evaluated in this paper are by anybody's standards quite good in comparison to what one might expect given these confines and constraints.

VII. SUMMARY AND CONCLUSIONS

The discussion above has presented an evaluation of VAS sounding data from three different retrieval algorithms in order to determine the accuracy and representativeness of the satellite sounding products as reflected by one case study. The verifying data consisted of special rawinsonde data having similar spatial resolution to that available from VAS. Special procedures were performed which interpolated the rawinsonde data to the satellite scan time and provided thermodynamic parameters at the

same locations for each data set. These procedures produced rawinsonde and satellite data valid at the same times at all pressure levels, grid point values over the same mesoscale domain, and analyses which allowed for the same potential for detail in each data field.

Mean and standard deviations of the difference between the rawinsonde and satellite grid point values are very useful in determining biases and errors in the data. In the all-time average, large temperature and moisture biases exist for all three retrieval sets at levels where inversions are prominent. Differences do exist between the various retrieval sets, particularly when the time variability is considered. It is difficult to say which of the three retrieval schemes is best since none of them consistently describe the mesoscale environment better than the others. The two physical schemes tend to produce soundings which are too moist while the regression moisture retrievals are almost unbiased. As a measure of error in the VAS retrievals, standard deviation of the difference between the satellite values and the ground truth were evaluated. In most cases the standard deviations were largest in the upper levels. Values ranged from $1°$ to $2°C$ for temperature and $3°$ to $5°C$ for dewpoint for each retrieval scheme.

Derived parameters from the VAS soundings reflect the biases in the original temperature and moisture profiles to a large extent. Geopotential height profiles are generally good especially for the modified physical retrievals, while heights become too large in the upper levels from the regression and physical retrievals. Standard deviations for the height values range from 20 to 30 m above 600 mb and somewhat smaller below this level.

The horizontal gradients, as defined by the VAS data, are generally weaker than those of the rawinsonde. Temperature gradient differences of $1°C/100$ km are not uncommon at various levels. In some cases the mesoscale gradients are not properly orientated with that of the rawinsonde.

An evaluation of the first guess information indicates that very little improvement is made in the vertical structure over that of the first guess information. Significant improvement is made in the horizontal structure over that provided by the first guess data, however. There seems to be some dependence in the two physical retrieval sets on this information and may explain the disorientation of the gradients, particularly in the middle and upper levels.

The errors and discrepancies highlighted in this paper can be attributed to a number of phenomena. First, the rawinsonde data are not error free and may account for some of the differences, especially in the dewpoint comparisons. However, the major cause for disagreement is due to sampling differences between the two types of measurements. The satellite radiance measurements represent a volumetric average of the temperature and moisture distribution while the rawinsonde is virtually a point measurement. This tends to reduce the resolving power of the VAS instrument and limits the amount of vertical information recoverable by any retrieval method. The spatial averaging from a single field of view (performed to increase the signal-to-noise ratio) increases the horizontal information content and thereby produces a smoother representation of the mesoscale environment.

REFERENCES

1. Anthony, R. W. and Wade, G. S.: VAS Operational Assessment Findings for Spring 1982/83. Thirteenth Conf. on Severe Local Storms, AMS, Boston, 1983, pp. J23-J28.

2. Menzel, W. P., Smith, W. L., and Herman, L. D.: VAS Radiometric Calibration: An Inflight Evaluation from Intercomparisons with HIRS and Radiosonde Measurements. Appl. Opt., Vol. 20, 1981, pp. 3641-3644.

3. Chesters, D. L. W. Uccellini, and Mostak, A.: VISSR Atmospheric Sounder (VAS) Simulation Experiment for a Severe Storm Environment. Mon. Wea. Rev., Vol. 110, No. 3, 1982, pp. 198-216.

4. Lee, T-H., Chesters, D., and Mostek, A.: The Impact of Conventional Surface Data Upon VAS Regression Retrievals in the Lower Troposphere. J. Clim. Appl. Meteor., Vol. 22, 1983, pp. 1853-1874.

5. Smith, W. L.: The Retrieval of Atmospheric Profiles from VAS Geostationary Radiance Observations. J. Atmos. Sci., Vol. 40, 1983, pp. 2025-2035.

6. Chesters, D., Uccellini, L. W., and Robinson, W. D.: Low-Level Water Vapor Fields from the VISSR Atmospheric Sounder (VAS) "Split Window" channels. J. Clim. Appl. Meteor., Vol. 22, 1983, pp. 725-743.

7. Petersen, R. A., Uccellini, L. W., Mostek, A., and Keyser, D.: The Use of VAS Channels in Delineatting Regions with a Potential for Convective Instability. Accepted by Bull. Amer. Meteor. Soc., 1984.

8. Smith, W. L., and Zhou, F. X.: Rapid Extraction of Layer Relative Humidity, Geopotential Thickness, and Atmospheric Stability from Satellite Sounding Radiometer Data. Appl. Opt., Vol. 21, 1982, pp. 924-928.

9. Hill, C. K., and Turner, R. E.: NASA's AVE/VAS Program. Bull. Amer. Meteor. Soc., Vol. 64, 1983, pp. 796-797.

10. Smith, W. L., Soumi, V. W., Menzel, W. P., Woolf, H. M., Sromovsky, L. A., Revercomb, H. E., Hayden, C. M., Erickson, D. N., and Mosher, F. R.: First Sounding Results from VAS-D. Bull. Amer. Meteor. Soc., Vol. 62, No. 2, 1981, pp. 232-236.

11. Smith, W. L.: Iterative Solution to the Radiative Transfer Equation for the Temperature and Absorbing Gas Profile of an Atmosphere. Appl. Opt., Vol. 9, 1970, pp. 1993-1999.

12. Smith, W. L.: An Improved Method for Calculating Tropospheric Temperature and Moisture from Satellite Radiation Measurements. Mon. Wea. Rev., Vol. 96, 1968, pp. 387-396.

13. Sienkiewicz, M. E.: AVE/VAS II: 25 mb Sounding Data. NASA CR-170691, Marshall Space Flight Center, Huntsville, Alabama, 1982, 303 pgs.

14. Fuelberg. H. E., and Jedlovec, G. J.: A Sub-synoptic-scale Kinetic Energy Analysis of the Red River Valley Tornado Outbreak (AVE-SESAME I). Mon. Wea. Rev., Vol. 110, 1982, pp. 2005-2024.

15. Fuelberg, H. E.: Reduction and Error Analysis of the AVE II Pilot Experiment Data. NASA CR-120496, Marshall Space Flight Center, Huntsville, Alabama, 1974, 140 pp.

16. Bruce, R. F., Duncan, L. D., and J. H. Pierluissi: Experiment Study of the Relationship Between Rawinsonde Temperatures and Satellite Derived Temperatures. Mon. Wea. Rev., Vol. 105, 1977, pp. 493-496.

1. REPORT NO. NASA TP-2425	2. GOVERNMENT ACCESSION NO.	3. RECIPIENT'S CATALOG NO.		
4. TITLE AND SUBTITLE An Evaluation and Comparison of Vertical Profile Data From the VISSR Atmospheric Sounder (VAS)		5. REPORT DATE January 1985		
		6. PERFORMING ORGANIZATION CODE		
7. AUTHOR(S) Gary J. Jedlovec		8. PERFORMING ORGANIZATION REPORT #		
9. PERFORMING ORGANIZATION NAME AND ADDRESS George C. Marshall Space Flight Center Marshall Space Flight Center, Alabama 35812		10. WORK UNIT NO. M-474		
		11. CONTRACT OR GRANT NO.		
12. SPONSORING AGENCY NAME AND ADDRESS National Aeronautics and Space Administration Washington, D.C. 20546		13. TYPE OF REPORT & PERIOD COVERED Technical Paper		
		14. SPONSORING AGENCY CODE		

15. SUPPLEMENTARY NOTES

Prepared by Systems Dynamics Laboratory, Science and Engineering Directorate.

16. ABSTRACT

A statistical evaluation is used to compare vertical profiles of temperature and moisture derived from VAS with three different algorithms to that of corresponding rawinsonde measurements for a clear-cold environment. To account for time and space discrepancies between the data sets, rawinsonde data were adjusted to be representative of the satellite sounding times. Both rawinsonde and satellite sounding data were objectively analyzed onto a mesoscale grid. These grid point values were compared at 50 mb pressure increments from the surface up to 100 mb. The data were analyzed for horizontal and vertical structure, representativeness of derived parameters, and significant departure (improvement) from the apriori (first guess) information.

Results indicate some rather strong temperature and moisture biases exist in the satellite soundings. Temperature biases of 1° to 4°C and dewpoint biases of 2° to 6°C generally occur in layers where strong inversions are present and vary with time as these atmospheric features evolve. The biases also change as a function retrieval scheme suggesting limitations and restrictions on the applications of the various techniques. Standard temperature deviations range from 1° to 2°C for each retrieval scheme with maximum values around 800 and 400 mb. Derived parameters (precipitable water and thickness) suffer from similar biases, though to a somewhat lesser extent. Gradients of basic and derived parameters are generally weaker but have good horizontal structure where magnitudes of the parameters are relatively strong. Integrated thermal (temperature) and moisture (precipitable water) parameters show mixed results. Although biases are small in the precipitable water values from the regression scheme, horizontal structure is poor.

An analysis of apriori and first guess information show similar biases when compared to the ground truth measurements. This information, however, seems to provide the majority of the vertical structural information present in the VAS retrievals.

17. KEY WORDS Atmospheric Science Satellites Sensors Meteorology	18. DISTRIBUTION STATEMENT Unclassified — Unlimited STAR Category: 47 and 35		
19. SECURITY CLASSIF. (of this report) Unclassified	20. SECURITY CLASSIF. (of this page) Unclassifed	21. NO. OF PAGES 38	22. PRICE A03

NASA